US Department of Energy
FreedomCAR and Vehicle Programs

Innovative Structural and Joining Concepts for Lightweight Design of Heavy Vehicle Systems

Contract No. EE50692

FINAL REPORT

Jacky C. Prucz. Ph.D.
Samir N. Shoukry, Ph.D.
Gergis W. William, Ph.D., P.E.

Department of Mechanical and Aerospace Engineering
College of Engineering and Mineral Resources

West Virginia University

August 2005

TABLE OF CONTENTS

LIST OF FIGURES

LIST OF TABLES

CHAPTER ONE

INTRODUCTION

1.1   Background

Recent advances in the area of Metal Matrix Composites (MMC's) have brought these materials to a maturity stage where the technology is ready for transition to large-volume production and commercialization. The new materials seem to allow the fabrication of higher quality parts at less than 50 percent of the weight as compared to steel, especially when they are selectively reinforced with carbon, silicon carbide, or aluminum oxide fibers. Most of the developments in the MMC materials have been spurred, mainly by applications that require high structural performance at elevated temperatures, the heavy vehicle industry could also benefit from this emerging technology. Increasing requirements of weight savings and extended durability are the main drivers for potential insertion of MMC technology into the heavy vehicle market. Critical elements of a typical tractor – trailer combination, such as highly loaded sections of the structure, engine components, brakes, suspensions, joints and bearings could be improved through judicious use of MMC materials. Such an outcome would promote the DOE's programmatic objectives of increasing the fuel efficiency of heavy vehicles and reducing their life cycle costs and pollution levels. However, significant technical and economical barriers are likely to hinder or even prevent broad applications of MMC materials in heavy vehicles. The tradeoffs between such expected benefits (lower weights and longer durability) and penalties (higher costs, brittle behavior, and difficult to machine) must be thoroughly investigated both from the performance and cost viewpoints, before the transfer of MMC technology to heavy vehicle systems can be properly assessed and implemented. MMC materials are considered to form one element of the comprehensive, multi-faceted strategy pursued by the High Strength / Weight Reduction (HS/WR) Materials program of the U.S. Department of Energy (DOE) for structural weight savings and quality enhancements in heavy vehicles.

1.2   Objectives

The research work planed for the first year of this project (June 1, 2003 through May 30, 2004) focused on a theoretical investigation of weight benefits and structural performance tradeoffs associated with the design, fabrication, and joining of MMC components for heavy-duty vehicles.

This early research work conducted at West Virginia University yielded the development of integrated material-structural models that predicted marginal benefits and significant barriers to MMC applications in heavy trailers. The results also indicated that potential applications of MMC materials in heavy vehicles are limited to components

identified as critical for either loadings or weight savings. Therefore, the scope of the project was expanded in the following year (June 1, 2004 through May 30, 2005) focused on expanding the lightweight material-structural design concepts for heavy vehicles from the component to the system level. Thus, the following objectives were set:

- Devise and evaluate lightweight structural configurations for heavy vehicles.
- Study the feasibility of using Metal Matrix Composites (MMC) for critical structural components and joints in heavy vehicles.
- Develop analysis tools, methods, and validated test data for comparative assessments of innovative design and joining concepts.
- Develop analytical models and software for durability predictions of typical heavy vehicle components made of particulate MMC or fiber-reinforced composites.

This report summarizes the results of the research work conducted during the past two years in this projects.

CHAPTER TWO

TECHNOLOGY ASSESSEMENT FOR MMC APPLICATIONS
IN HEAVY VEHICLES

2.1   Introduction

High-performance Metal Matrix Composite (MMC) materials are considered to form one element of the comprehensive, multi-faceted strategy pursued by the High Strength / Weight Reduction (HS/WR) Materials program of the U.S. Department of Energy (DOE) for structural weight savings and quality enhancements in heavy vehicles. A preliminary investigation of the potential benefits and barriers of using particulate MMC materials for selected structural components of heavy trailers is currently performed by West Virginia University (WVU), as part of the HS /WR Materials program. The overall scope of the WVU project, titled "Structural Characterization and Joining of MMC Components for Heavy Vehicles", is to quantify the cost-performance tradeoffs associated with the development of MMC components for heavy trailers, while also devising innovative design and joining concepts for enhancing such tradeoffs. The main objective of this document is to summarize and report the findings generated by the WVU effort so far, under Task I of the project: "**Updated Assessment of the Current State-Of-The-Art of Technology Development and Commercial Applications for Advanced MMC Materials".** The main goal of collecting and analyzing the information for this task is to identify the most critical needs and opportunities, along with the most appropriate strategies for reducing the structural weight and the life cycle costs of heavy vehicles, with emphasis on MMC materials and heavy trailers.

2.2   Information Sources

Five primary resources of information have been utilized to compile data about the current technical knowledge, user requirements, regulations, materials, design and manufacturing technology for heavy vehicles:

1. Direct interactions with representatives from the DOE, national laboratories, and the heavy vehicle industry, including Original Equipment Manufacturers (OEM), first-tier suppliers and materials suppliers, especially during the Workshop on a "Research and Development Plan for High Strength/Weight Reduction Materials", hosted by the Oak Ridge National Laboratory (ORNL) on April 24-25, 2002 [1].

2. Direct communications with senior-level engineers from the Great Dane Trailers Company, and site visits at two of its facilities: (a) the maintenance center in

Richmond /Virginia, in October 2002 and (b) the research and development center in Savannah / Georgia, in December 2002.

3. Public domain literature, including Internet web sites, related to structural aspects of national standards, industry regulations, methods, tools and data that govern the design, production, testing and service procedures of heavy vehicles [2].

4. Technical reports of government [3] or industrial [4] task forces, that document earlier investigations of Research and Development (R&D) needs, marketing opportunities, application barriers, challenges and strategies of advanced materials in general [3], and MMC materials in particular [4].

5. Descriptions of technical patents issued during the last five years by the U.S. Patent Office for innovations related, primarily, to the construction and assembly of composite structural parts for heavy trailers [5].

2.3 Lightweight Structures for Heavy Vehicles

The heavy-duty vehicles referred to in this study include highway trucks and buses categorized as Classes 2C through 8. The total production volume for Classes 3 through 8 in year 2000 was about 565,000 new vehicles, of which 88.5% are powered by Diesel engines [6]. The average fuel efficiency of a heavy vehicle is 6 miles per gallon (mpg), and a total of 18 billion gallons of fuel are estimated to be burned annually by a fleet consisting, approximately, of about 1.7 million tractor/trailer combinations [7]. Any significant reduction in the structural weight of such a vehicle is likely to not only improve its fuel efficiency by reducing the parasitic energy losses, but also decrease the level of exhaust emissions by lowering the power output required for given driving conditions. A recent study conducted by an industrial team for the Canadian "Transportation Development Centre" [8] estimates that a 9% weight reduction in the structure of an intercity bus would reduce the 15-year fuel costs for such a bus by 4.5%, whereas a 20% weight reduction could reduce the 15-year fuel expenditures by 10%. Additional benefits enabled by weight reductions of 9% and 20%, are lower pollutant emissions, lower maintenance costs for the bus fleet and for the road infrastructure, totaling to 15-year Life-Cycle-Cost (LCC) savings of 3% and 6.7%, respectively.

A combination of economical-structural-material considerations must underlie any comprehensive, system-level study of potential weight reductions in a heavy vehicle. Such an investigation would commence, usually, with identifying the heaviest assemblies or sections in a typical vehicle, where any reduction in structural weight is likely to impact significantly the overall weight of the vehicle. This is the strategy described both in References [6] and [8], though the focus of the analysis is a certain type of vehicle in Reference [8], namely a intercity bus, whereas the central goal of the study reported in Reference [6] is to explore application opportunities for a certain type of material, namely titanium, in suitable components of any heavy vehicle. The most promising design concepts for weight reductions in intercity buses are based on sandwich panel

construction using foam cores with skins made of either Aluminum or fiberglass [8]. The application of a new material in a heavy-duty vehicle has to be driven either by the potential of emissions reduction, weight reduction, or certain unique material properties [6]. Despite their light weight, high specific strength, high temperature performance, good toughness and corrosion resistance, titanium materials are unlikely candidates for high-volume applications in heavy vehicles, since they are heavier than materials presently used in cab sections (aluminum, polymer composites), and they are too expensive for body and chassis systems [6]. "Bulk haul" carriers run their vehicles at maximum certified weight, so that each pound saved in structural weight would translate into an additional pound of cargo. It is reasonable to ascertain that a typical operator would be ready to pay a premium of about $3-4 for every additional pound of cargo, which implies that the target market cost of a titanium alloy must not exceed $4-5 /lb., which is an unrealistic expectation for such material. Therefore, low-cost, high-performance titanium materials are viable for certain engine and suspension components, but not for large body or chassis structures [6]. It is logical to assume that a similar study directed towards applications of MMC materials in heavy vehicles may lead to similar conclusions as for the case of titanium alloys.

A wide variety of innovative design and manufacturing concepts, combined with selective applications of polymer composites, light-weight metals and wood materials, have been implemented in the last decade to reduce the structural weight and improve the overall quality of certain heavy vehicle systems. Numerous U.S. patents have been issued during this period in connection with the manufacturing of composite assemblies for heavy-duty trailers, and effective joining configurations between different composite parts [5]. Successful case studies of specific solutions to weight reductions in heavy-duty vehicles have been reported in the past with regard to Diesel engines [9], driveshafts made of carbon-fiber composites [10], as well as lightweight system-level specifications, design, and production of tractor-trailer systems [11]. The payoffs of a consistent formal weight reduction program are reflected well in the example of the Petroleum Transport of Illinois, Inc., which embarked on such an initiative in 1990, and succeeded to gain a competitive edge in its market with vehicles lighter by about 385 lb., with a payload capacity of 56,000 pounds [11]. Most efforts pursuing the migration of lightweight materials technology to heavy-duty vehicles have been directed so far towards light metals (aluminum, magnesium, titanium), carbon and polymer-matrix composites (PMC). A relatively new class of materials that provides the potential for significant weight savings at affordable costs is that of metal foams, which could be used in automotive structures either as self-contained components or in the form of sandwich cores [12]. Although their processing and design methodologies are not, yet, fully developed and controlled, ultra-light aluminum foams, for example, are extremely attractive for lightweight construction of trucks and trailers, since they offer high specific stiffness, good thermal management, good acoustic and electric properties, high energy absorption, and, therefore, good crash resistance [13]. Moreover, some metal foams seem to be inexpensive and suitable for low-cost, large-volume applications.

2.4   Metal-Matrix Composite (MMC) Materials

Metal matrix composite materials are formed, usually, of a low-density metal alloy, such as aluminum or magnesium, reinforced with particles, whiskers, or fibers of a ceramic material, such as silicone carbide or graphite. Their performance is superior to that of the unreinforced metal, especially with respect to higher specific strength and stiffness, higher operating temperatures, and greater wear resistance. The disadvantages of MMC materials are related, mainly, to their high cost and complex manufacturing processes, though two of their drawbacks relate also directly to their mechanical properties, namely lower ductility and lower toughness than corresponding, unreinforced metals [3]. The primary market for MMC materials is in military and aerospace applications, for high performance systems such as jet engines, missiles, satellites, and the Space Shuttle. Commercial applications are still rather limited, and they range from selected automotive components, such as pistons, connecting rods, brake rotors and drums, to electronic devices, electrical circuit breakers, and even sporting goods such as tennis rackets and bicycles.

For any given combination of its fiber and matrix constituent materials, the thermal, mechanical, and electrical properties of a MMC system can be tailored to specific application requirements by controlling the length-to-diameter ratio of the fibers. Continuously reinforced MMC's correspond to large values of this ratio, which lead to superior mechanical properties, but higher material costs and more expensive and difficult processing methods. Discontinuously reinforced, or particulate, MMC materials are characterized by small length-to-diameter ratios of the reinforcement, which could be in the form of chopped fibers, particles, or whiskers [4]. This class of MMC's are suitable for low-cost, low-performance applications, such as in certain automotive components, since they are easier to process, and they exhibit essentially isotropic behavior, but with substantial strength, stiffness, thermal resistance and wear improvements, in comparison with unreinforced metals. Although their mechanical properties are superior to those of equivalent metals, and although they are more affordable than continuously reinforced MMC's, discontinuously reinforced MMC material have not been applied, yet, in large volumes for major, load carrying components in aerospace, automotive, industrial, road or maritime structures.

The principal impediment to high-volume applications of MMC materials is their overall cost, which depends on each of the main four stages forming the life-cycle of such a material:

1) Raw material costs,
2) Manufacturing processes,
3) Machining or second fabrication, and
4) Service conditions.

Raw material costs are very sensitive to the production volumes, though certain materials are inherently expensive and will never be cheap enough for widespread commercial use; the cost of certain ceramic fibers, for example, may run as high as

$1,000 per pound, which cannot, obviously, compete against the cost of $20 per pound of high quality Kevlar 49 fibers or Carbon/Epoxy Nomex composite laminates. The production processes of MMC's remain their primary avenue to significant cost reductions, both at the stage of primary processes, where the MMC material is formed through combining and consolidating operations, and at the stage of secondary processes, which consists mostly of shaping and joining operations. Net-shape manufacturing methods are especially important for MMC materials, both in order to reduce the scrap of expensive constituents, and to reduce the need for expensive machining operations. Other major impediments to broad commercialization of MMC materials in general, and their utilization in major structural components of heavy vehicles, are outlined below [4]:

- Lack of large-volume commercial applications
- Lack of effective design and analysis techniques, which cannot be developed without standardized testing procedure, federal and industry standards, reliable analytical models, extensive, accessible database of MMC material properties.
- Mismatch of thermal expansion coefficients at the fiber-matrix interfaces.
- Lack of reliable non-destructive evaluation (NDE) techniques for quality control, product acceptance criteria, testing standardization and automation.
- Lack of verified techniques for damage repair, especially delaminations, debonding of fiber-matrix interfaces, and broken fibers.
- Lack of regulated procedures for recycling MMC scrap.

2.5   Summary

A combination of economical factors and technological gaps are still hindering, to this date, widespread applications of MMC materials, beyond their selective use in high-performance components or non-structural devices. Only the discontinuously reinforced class of MMC materials can be considered today a viable candidate for applications in heavy vehicle structures, provided that their initial costs can be reduced to affordable levels for the trucking industry, and practical methods are devised for their repairs in the field, as well as secondary fabrication processes, i.e. shaping and joining. The most common materials used as reinforcements in such metal-matrix composites, either in the form chopped fibers, whiskers, flakes or particulates, are alumina, graphite, carbon, magnesium, silicon, tungsten, titanium, boron carbides, or silicon, aluminum, titanium nitrites. The common types of matrix materials used in discontinuously reinforced MMC's are aluminum, magnesium, copper and zinc. The taxonomy of primary processing methods of discontinuously reinforced MMC materials includes casting, powder metallurgy, infiltration, hot isostatic pressing, and ingot metallurgy, complemented by secondary fabrication methods such as recasting, forging, extrusion, milling, machining, joining and welding [4]. Current application examples of discontinuously reinforced MMC's span over a variety of commercial markets, such as heavy-duty vehicles (pistons, cylinder liners in Diesel engines, brake rotors, brake drums), transmission components (worm gears, bearings, truck drive shafts), electronics

racks and packaging, sporting goods (bicycle frames, golf club heads), precision optical instruments, and aerospace structures (vertical stabilizers of aircraft, for example).

The thermo-mechanical properties of discontinuously reinforced MMC's depend not only on the particular material constituents and processing techniques used for their fabrication, but also on the volume fraction and the length-to-diameter ratio of their reinforcements. The strength and stiffness characteristics of a given combination of material constituents can be enhanced significantly by increasing the volume fraction of the reinforcement, as illustrated in Figure 2.1 for the particular case of a 6091 Aluminum Alloy reinforced by Silicon Carbide particles. Unfortunately, these benefits come at the expense of higher costs and more difficult fabrication processes.
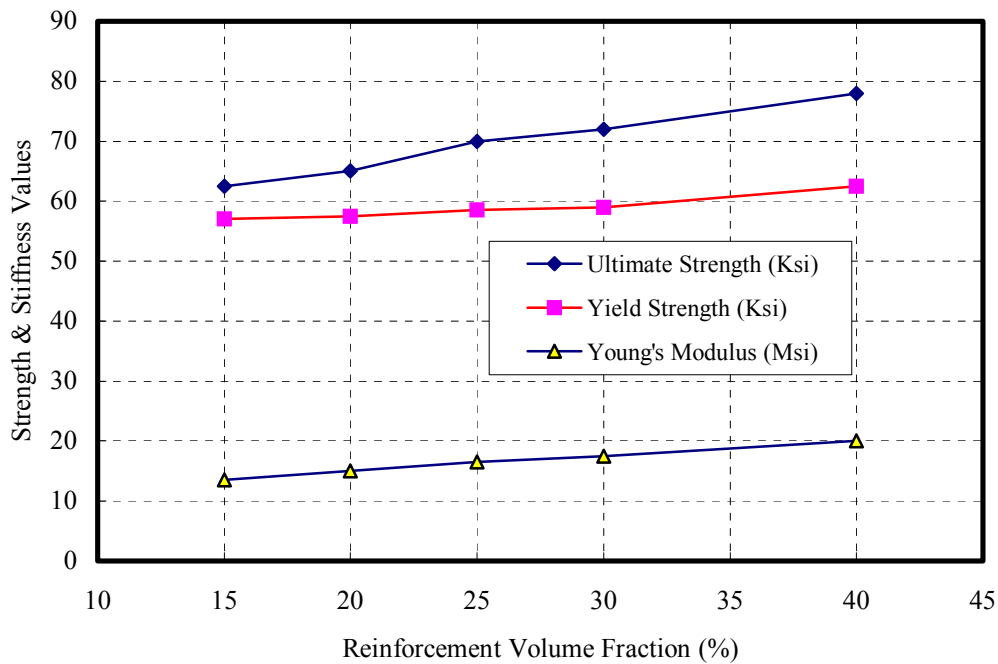
Figure 2.1 - The Effects of Percentage Reinforcement on Mechanical Properties of a Material System Consisting of 6091 Aluminum Alloy and Silicon Carbide Particles

The primary advantage of MMC materials is the potential for higher ratios between their strength or stiffness properties and their densities, than those achievable with competing metal or polymer-based composites, as indicated, for exemplary comparison, by the specific strength and stiffness values shown in Table 2.1.

Table 2.1 Typical Properties of Discontinuously Reinforced MMC's and Other Material Systems

Material System	Specific Strength, 10^3m	Specific Stiffness, 10^6m
Steel	12.92	2.71
Aluminum Alloy	10.57	2.68
SiC Ceramic	15.61	9.88
S-Glass PMC* Laminate	27.56	2.86
Carbon PMC Laminate	36.82	8.47
2000 Series Al Matrix + 25% SiC whiskers	225	37
7000 Series Al Matrix + 25% SiC whiskers	300	42

*PMC – Polymer Matrix Composite.

Other performance drivers for commercialization of MMC materials are [14]:

- Higher fatigue strength than un-reinforced metals.
- Ability to tailor the material properties to specific application requirements.
- Good damping capacity and potential to control noise and vibration levels.
- High-temperature capability, beyond that achievable with polymer-matrix composites.
- Good resistance to wear and environmental conditions.
- Easy joining by conventional means, especially for discontinuously reinforced metal-matrix composites.

High costs due to low production volumes, insufficient characterization data, lack of reliable models and standardized design, manufacturing and testing methods, remain to this date the major barriers to widespread commercialization of MMC materials. It is highly unlikely that drastic weight reductions can be achieved in heavy vehicle structures by using such materials. Continuously reinforced MMC's are unlikely to be economically feasible for the trucking industry, whereas discontinuously reinforced MMC's are attractive only for limited, low-volume applications, in selected components of a tractor-trailer system, where their technical advantages are critical, evident, and justify the replacement of existing materials. Any insertion of a new material system into the load carrying structure of a heavy vehicle must rely on a comprehensive, life-cycle analysis of multiple alternatives; in the context of an integrated design approach that yields the best possible match between the material properties and the geometric or assembly characteristics of the structure.

CHAPTER THREE

WEIGHT COMPARISON FOR CROSS BEAMS
IN CHASSIS OF HEAVY VEHICLES

3.1 Mass Distribution in Current Design Configuration

A detailed 3D Finite Element model of a typical "Box Trailer" has been developed by using a combination of thin shell and beam elements. It relies on the design drawings provided by Great Dane Trailer Company for commonly used lengths of 48, 54 and 58 feet for such box trailers. All the substructure assemblies of the trailer have been included in the model. Figure 3.1 shows the finite element mesh used to model such a trailer.
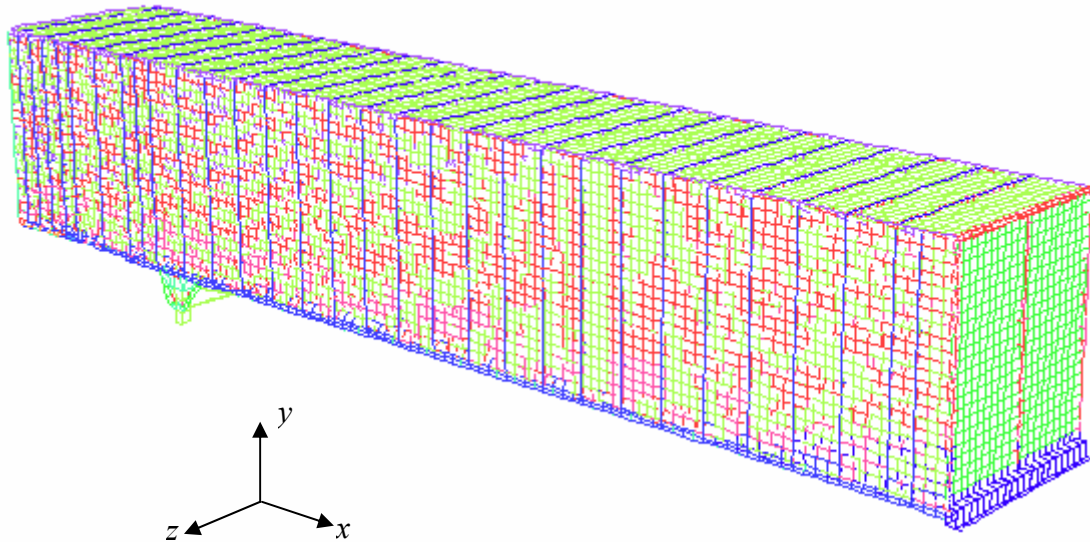
Figure 3.1 3D Finite Element Model of a Van-Trailer.

Based on the current design, the box trailer was divided into four sections, as shown in Figure 3.2. Weight calculations have been conducted based on this model in order to determine the centers of gravity and weight distributions of trailers of different lengths, for the conventional steel and aluminum materials employed in current designs. The results are summarized in Table 3.1.
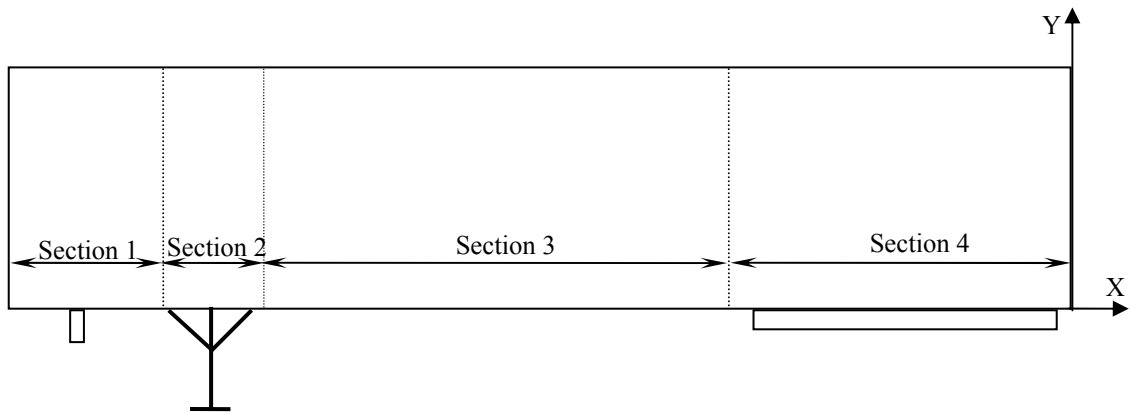
Figure 3.2 Layout of a Typical Box Trailer.

For a better simulation, a suspension model will be added to the trailer model. The trailer will be loaded with a cargo weight. The trailer will be loaded to evaluate the global flexural and tensional stiffness. The finite element model will be used to compare between alternative material selections (aluminum, steel, MMC, carbon-carbon composites for different parts on the global structural stiffness of the trailer structure and its overall weight.

TABLE 3.1 Mass and center of gravity of Trailers

Section #	Length (m)	Mass (kg)	X(m)	Y(m)	Z(m)
Mass distribution for 48' trailer					
1	2.629	1523	-13.41	0.3854	0
2	1.541	455	-10.11	0.568	0
3	5.883	1550	-6.394	0.5789	0
4	4.573	1752	-0.9095	0.5348	0
Total	14.63	5281	-6.78	0.512	0
Mass distribution for 54' trailer					
1	2.771	1509	-14.22	0.3854	0
2	1.829	613	-11.71	0.3315	0
3	6.706	1895	-7.699	0.4921	0
4	4.924	2034	-1.118	0.4621	0
Total	16.3	6050	-7.42	0.4385	0
Mass distribution for 58' trailer					
1	2.771	1509	-15.43	0.3854	0
2	1.829	626	-12.99	0.355	0
3	8.047	1958	-7.989	0.4855	0
4	4.973	2243	-1.369	0.4639	0
Total	17.62	6336	-7.971	0.4398	0

11

3.2   Estimating the Weights of Different Trailer's Components

The 3D finite element model developed in this study has also been used to estimate the weights of different components in order to identify the heavy components that would require a re-design in the process of reducing the weight of the current design configuration. The van-trailer structure is divided into two main parts:
1. Chassis assembly
2. Sides and roof

The volumes and masses of the components of each main part are listed in Tables 3.2 and 3.3 for the 48-foot length van-trailer. As can be indicated from Tables 3.2 and 3.3, the total weight of the van-trailer is 51,272 N (11,500 lb). This estimated weight agrees with the published values for empty trailers [].

Table 3.2   Masses of Chassis Parts

Part Name	Volume (m3)	Mass (kg)
Oak Floor (1.38" thick)	1.1370	503.3
I-beams	0.1350	1,058.0
Suspension Rail	0.0491	383.9
Front Bottom	0.0421	328.8
5th Wheel Channel	0.0279	218.3
Hat Beams	0.0266	207.6
Bumper	0.0169	131.9
Rear Side (Chassis Beam)	0.0462	125.4
Front top	0.0101	79.2
5th Wheel Top Plate	0.0100	78.2
Front Channel	0.0085	66.4
Floor Support	0.0044	34.2
Front Plate	0.0040	31.3
Landing Gear Mounting Angle	0.0034	26.4
Suspension Rail Stopper	0.0026	20.1
5th Wheel reinforcement	0.0024	18.9
Hat Sides (Chassis Beam)	0.0018	14.3
Landing Gear reinforcement	0.0010	8.1
Front Corners	0.0009	6.9
Front Sides	0.0029	2.3
Bracket (Side Chassis Beam)	0.00007	0.6
	Σ	3,344.1

The chassis assembly contributes about 64 percent of the overall weight of a typical 48-ft van trailer, of which 47 percent is contributed by the oak floor panels and the cross beams that support the floor. One set of such cross beams comprises simply supported I-beams evenly distributed at 0.305 m (1 ft) spacing along the central section of the van, whereas the other set consists of I-beams with overhanging cantilevers over

the suspension rail as illustrated in Figure 3.3. This indicates that the floor assembly has a great potential for weight saving through integrated material-structural analysis.

Table 3.3   Masses of Walls and Roof

Part Name	Volume (m3)	Mass (kg)
Skin	0.2000	542.5
Corner Beams	0.0027	7.4
Plywood Slides	0.8710	385.3
Side Post	0.0295	230.4
Top Rail	0.0490	132.9
Scuff Plate	0.2560	113.4
Rear Corner	0.0139	108.5
Roof Beams	0.0114	89.0
Rear Doors	0.1870	82.9
Rear Header	0.0056	43.5
Landing Gear Legs Bottom	0.0055	43.4
Frond Post	0.0044	24.2
Landing Gear Mounting Bracket	0.0030	23.3
Landing Gear K Brace	0.0018	14.3
Landing Gear Legs	0.0016	12.8
Landing Gear Diagonal Brace	0.0012	9.7
Door Frame	0.0019	5.2
King Pin Plate	0.0006	5.0
Landing Gear Feet	0.0005	3.9
Corner	0.0011	3.0
King Pin	0.0002	1.8
Σ		1,902.4

The chassis weight is carried directly by these cross beams as a uniformly distributed weight carried by each cross beam. The intensity of such a load can be determined as follows:

Beam own weight = 95 N/m
Weight of the oak floor = 0.036×0.305×(445*9.81) = 48 N/m

Therefore, total intensity of dead load = 143 N/m.

In the central zone, the ends of such beams are supported on the main floor frame that is carrying the loads from the side walls and the roof.

Over the rear axle of the trailer, the thirteen cross members supported over the sliding rail transmit the load from the main wall frame to the suspension rail. As

indicated from Table 3.3, the total load from the trailer walls and roof is 18,500 N (4,150 lb). This load is carried by the two sides of the trailer, thus the load on each sides is 9,250 N (2,075 lb). Such load is uniformly distributed over the entire length of frame (14.63 m), so the amount of such uniformly distributed load on each side wall is 632 N/m.
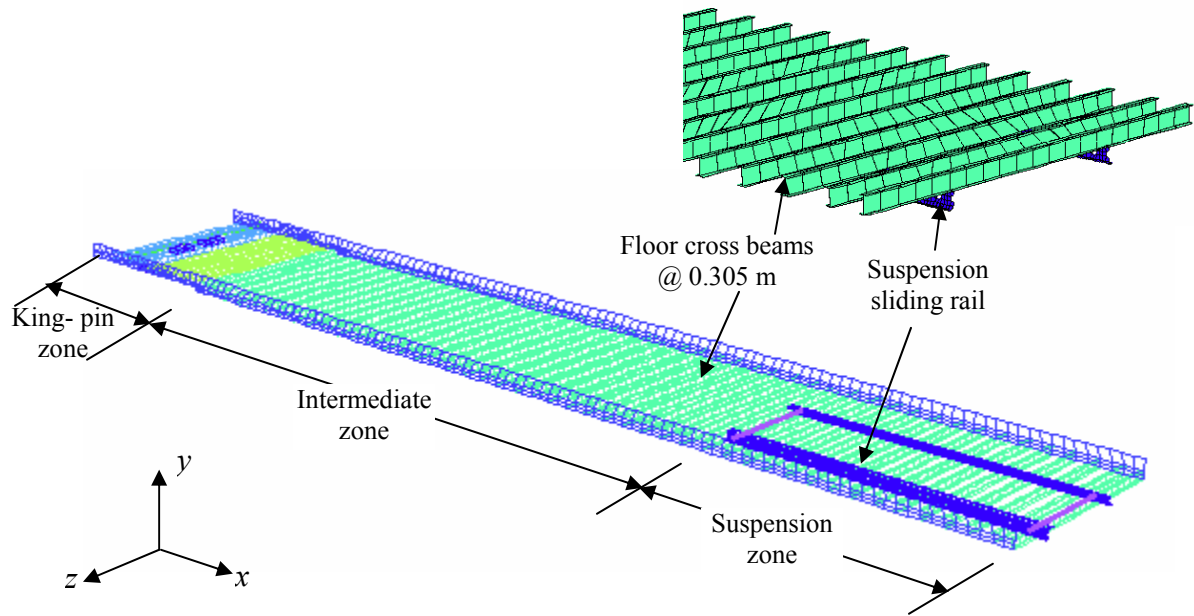
Figure 3.3 Floor Cross Beams.

The chassis contributes a uniformly distributed load of 143×2.6/ (2×0.305) = 609 N/m to each of the side wall frames. Therefore, the dead load distribution on the longitudinal frame is as shown in Figure 3.4. The structural system of the side walls and roof of a can-trailer is illustrated in Figure 3.5.
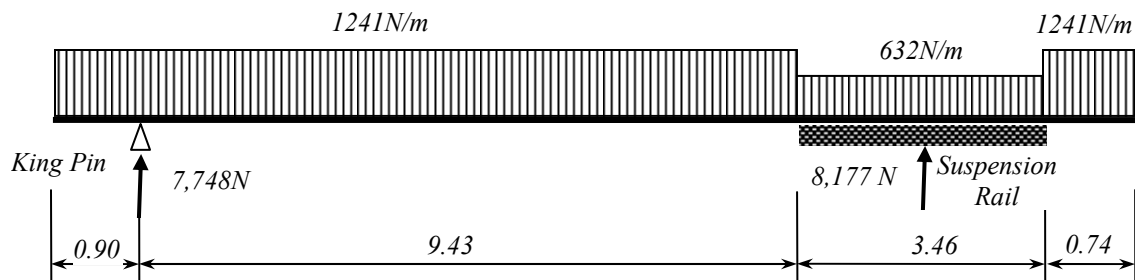
Figure 3.4. Load Distribution along the Side Frame.
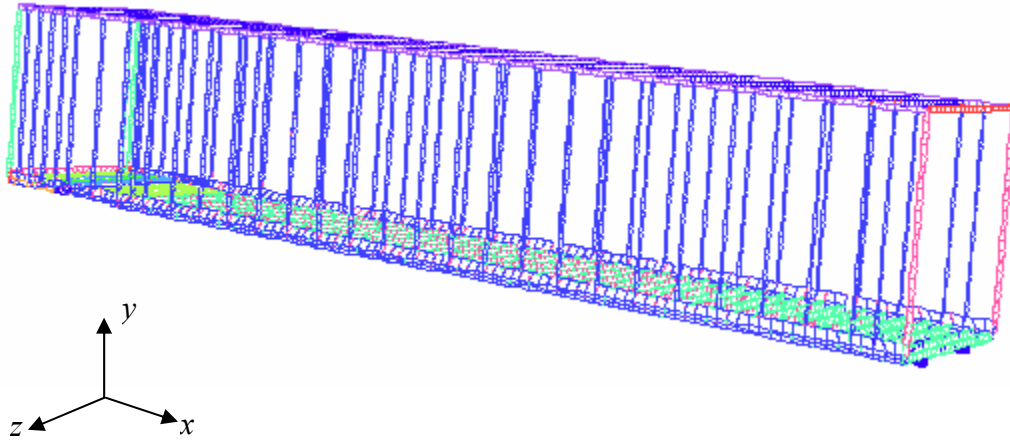
Figure 3.5 Structural System of the Trailer Sides and Floor.

3.3   Distribution of Dead Loads on Cross Beams

3.3.1   Simply Supported Cross Beams

These cross beams are in the middle zone of the chassis between the suspension rail and the king pin as illustrated in Figure 3.6. The dead load acting on such beams is

143 N/m

2.60 m

a. Load Distribution

186 N

186 N

b. Shearing Force Diagram

121 Nm

c. Bending Moment Diagram
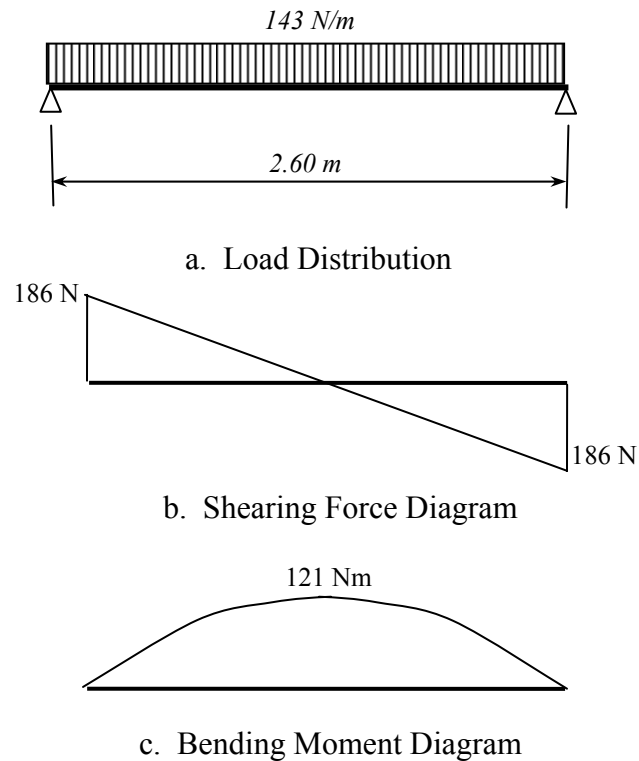
Figure 3.6 Straining Actions on an Intermediate Cross Beam due to Dead Load.

shown in Figure 3.6 (a). The distribution of the shearing force and bending moment due to such load are shown in figure 3.6 (b) and (c) respectively.

3.3.2 Cross Beams with Over-Hanging Cantilevers

These are the thirteen cross beams supported on the suspension rail, as can be seen in Figure 3.3. The distribution of the dead load over such beams is shown in Figure 3.7 (a). Each cantilever end is subjected to a concentrated load the value of which is equal to the load transmitted from the walls (8,177 N) divided by the number of cross members over the suspension slide rail (13 members). The distribution of the shearing forces and bending moment on this beam due to the dead load are shown in Figure 3.7 (b) and (c) respectively. Figure 3.7 (c) indicates that due to the concentrated loads acting on the cantilever edges, the entire span of the beam is subjected to negative bending moment, whose maximum values of 461 N.m occur above the supports. The presence of the over-hanging cantilevers made this type of beam critical in the design.

a. Load Distribution

b. Shear Force Diagram

c. Bending Moment Diagram
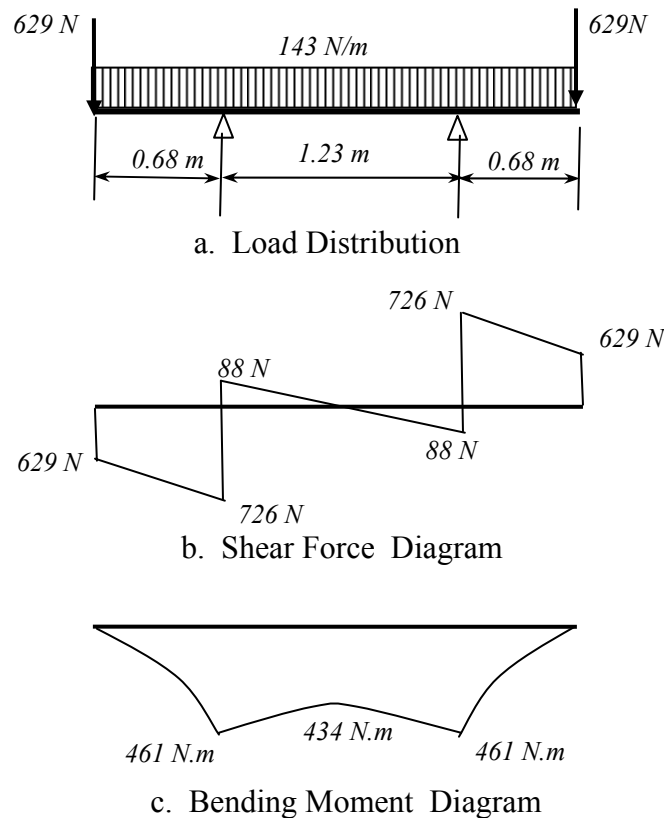
Figure 3.7 Straining Actions on a Cross Beam with Over-Hanging Ends
Due to Dead Load.

3.4   Live Load Distribution on Cross Members

Reviewing the current practice indicated that all trailers must be tested before operation by a passage of a loaded forklift over their floor beds.   In this study, we assume a baseline live load of a loaded forklift of a total weight of 44 kN (10 kips) carried over its four wheels. Therefore, each wheel is loaded by 11 kN (2,500 lb). The wheel spacing is 1.00 m.

3.4.1 Simply Supported Cross Beams

The critical loading position on a simply supported cross beam occurs when two wheels of the forklift rest symmetrically about the beam centerline as depicted in Figure 3.8 (a). Under such loading position, the distribution of the shearing forces and bending moment due to the live load is shown in Figures 3.8 (b) and (c).

a. Load Distribution

b. Shearing Force Diagram

c. Bending Moment Diagram
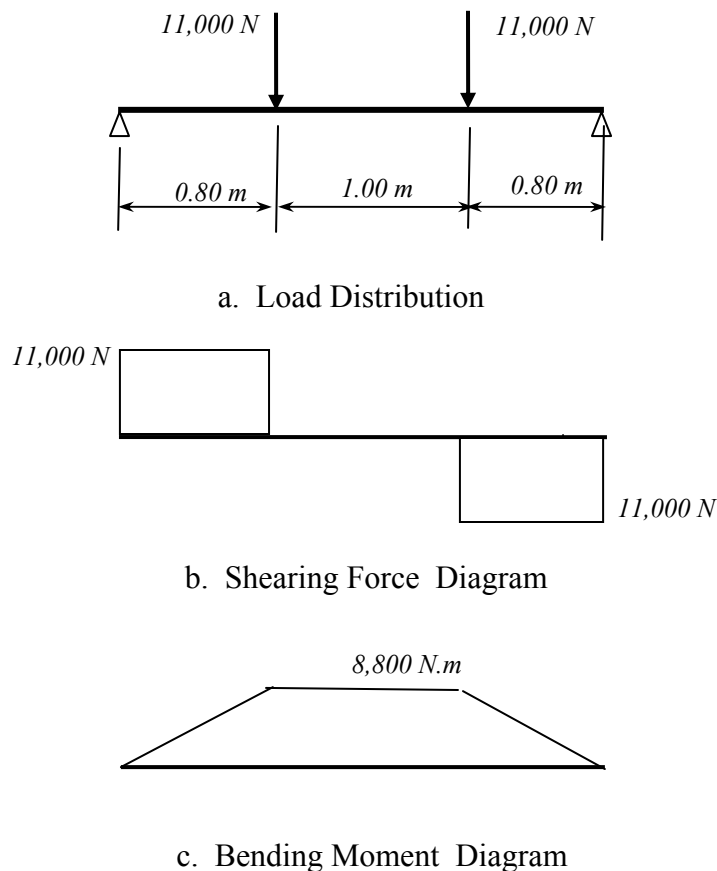
Figure 3.8 Straining Actions on a Simply Supported Cross Beam due to
Live Load.

3.4.2 Cross Beams with Over-Hanging Cantilevers

The critical loading position on a cross beam will occur when two wheels of the forklift rest on such cross beam as shown in Figure 3.9 (a). To facilitate the movement of the forklift, a clear distance of 0.22 m was assumed between the wheel and the side of the trailer. Under such loading position, the distribution of the shearing forces and bending moment due to the live load is shown in Figures 3.9 (b) and (c).
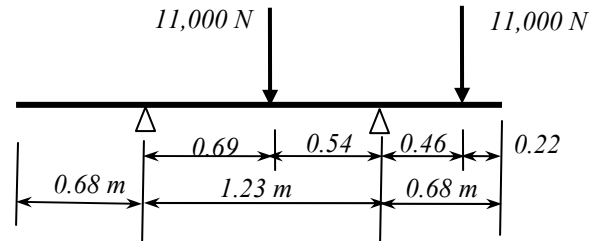
a. Load Distribution
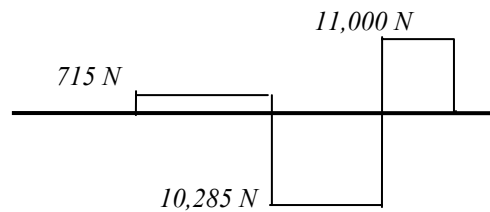
b. Shearing Force Diagram
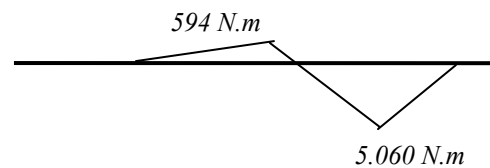
c. Bending Moment Diagram

Figure 3.9 Straining Actions on a Cross Beam with Over-Hanging Ends
Due to Live Load.

3.5 Loading Scenario and Critical Straining Actions in Baseline Design Configuration

The baseline loading scenario assumed to assess the current design configuration and for integrated structural design of the chassis components consists of structural dead loads as described in Section 3.3 and a live load applied by a moving 44 kN- forklift as described in Section 3.4. Due to such a loading scenario, the maximum straining actions on the steel I-cross beams are summarized as follows:

For simply supported cross beams:
     The maximum shear force = 186 + 11,000 (0.5+0.87) = 15,251 N
     The maximum bending moment = 121 + 8,800 = 8,921 N.m

For cross beams with overhanging cantilevers:
     The maximum shear force = 726 + 11,000 (0.19+1.00) = 13,783 N
     The maximum bending moment = 461 + 5,060 = 5,521 N.m

     Obviously, the simply supported cross members are more critical in design than those with overhanging cantilevers. As shown in Figures 3.3 and 3.5, standard I beam section is currently used for these cross members. The properties of the used cross section are:
     Nominal Size: 102 x 64 mm.
     Web thickness, t_w = 4.1 mm
     Flange thickness, t_f = 6.6 mm
     Cross sectional area, A = 12.3 cm^2
     Moment of inertia about x-axis, I_{xx} = 217.6 cm^4
     Moment of inertia about y-axis, I_{yy} = 25.3 cm^4
     First moment of area about x-axis, S_x = 25.48 cm^3
     First moment of area about y-axis, S_y = 6.95 cm^3
The beam is currently made of steel whose yield strength is 550 MPa (80 ksi).

Normal Stresses

Maximum bending moment = 8,921 N.m

$$Maximum\ Normal\ Stress = \frac{8,921 \times 0.051}{217.6 \times 10^{-8}} = 209\ MPa$$

Factor of safety = 550/209 = 2.63

Shear Stresses

Maximum Shear Force = 15,251 N

$$Maximum\ Shear\ Stress,\ \tau_{max} = \frac{Q_{max}\ S_x}{I_{xx}\ t}$$

$$\tau_{max} = \frac{15,251 \times 25.48 \times 10^{-6}}{217.6 \times 10^{-8} \times 0.041} = 4.36 MPa$$

The maximum allowable shear Stress = 0.5 σy = 275 MPa

Factor of safety = 275/4.36 = 63

Deflection Analysis

The analyses presented above indicate that the simply supported cross beam is more critical in design. Under the loading scenario defined in this study, the beam is symmetrically loaded for both dead load and live load. Thus, the maximum deflection occurs at mid-span. For the uniformly distributed dead load w, the mid-span deflection Δ_D can be calculated using the equation:

$$\Delta_D = \frac{5}{384} \frac{wl^4}{EI_{xx}}$$

For the two equal concentrated symmetrically placed wheel loads, the mid-span deflection can be calculated as:

$$\Lambda_L = \frac{Pa}{24 EI_{xx}} \left(3l^2 - 4a^2\right)$$

The total mid-span deflection is the sum of Δ_D and Δ_L. For the loading conditions illustrated in Figures 3.6 and 3.8, the mid-span deflections are:

Δ_D = 0.19 mm

Δ_L = 14.2 mm

Total mid-span deflection = 14.4 mm (0.56 inch).

3.6   Oak Floor

The current design configuration utilized floorboards of 36 mm (1.38 inches) laminated hardwood (oak boards) that are pre-undercoated and designed with a crusher bead joint to ensure a uniform and secure seal between the floor boards. The unit weight of such floorboard is 16 kg/m^2 (3.28 lbs/ft^2).

The structural function of these floorboards is to sustain the wheel loads from the moving forklift and transmit it to the adjacent cross beams. The bending moment develops in such boards due to the wheel load can be estimated as:

$$M = \frac{11{,}000 \times 0.305}{8} = 419 \text{ N.m}$$

The width of each of these boards is 0.3 m (11.9375 inches). Thus, the maximum flexural stress in such boards is:

$$\sigma = \frac{6 \times 419}{0.30 \times (0.036)^2} = 6.37 MPa$$

Factor of Safety = 20/6.37 = 3.14

3.7 Alternative Design Configuration Concepts of Cross Beams

Alternative design concepts for the structural floor of a van trailer were devised in order to reduce its weight below that of the current, baseline configuration. All these lightweight designs relied on sandwich or ribbed panels with various material and geometric characteristics of the core. The main design objective utilized in this comparative study was chosen to be an optimal tradeoff between the overall weight and stiffness of the floor. The following design criteria had to be met by all the alternative configurations considered here.

- The factor of safety in flexure should not be lower than 2.0.
- The mid-span deflection of a cross beam in an alternative, lightweight floor should not exceed that calculated for a similar steel beam currently used in the baseline floor configuration.

Alternative 1: The core of the floor consists of I-Cross beams made of various candidate materials, spaced at a distance of 1 ft apart as illustrated in Figure 3.10.
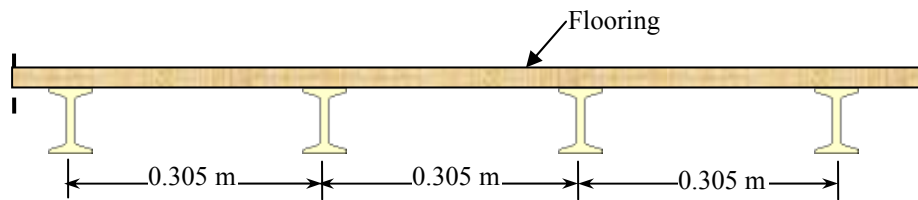
Figure 3.10 I-Cross Beam Floor.

TABLE 3.4 Alternative Material Solution for I-Beam Floor.

MATERIAL CANDIDATE	SIZE				Section Properties			Ultimate Strength	Flexural Stress	Factor of Safety	Mid-span Deflection	Weight
	d	bf	tw	tf	A	Ixx	S					
	mm	mm	mm	mm	cm²	cm⁴	cm³	MPa	MPa		mm	kg/m²
STEEL	102	64	4.1	6.6	12.3	217.6	42.8	550	208.43	2.64	14.40	31.61
Aluminum	204	58	3.4	4.8	12.387	770.03	75.71	240	117.83	2.04	12.04	31.73
EXTREN 525	204	102	9.5	9.5	36.97	2305.9	227	206	39.31	5.24	14.79	22.50
Carbon-Carbon	152	76	6	6	18.6	662	87.2	1096	102.31	10.71	7.00	9.65
Nitronic 19D Stainless Steel	102	64	4.1	6.6	12.3	217.6	42.8	714	208.43	3.43	14.61	31.15
Nitronic 60 Stainless Steel	102	64	4.1	6.6	12.3	217.6	42.8	1110	208.43	5.33	15.36	31.73
NItronic 30 Stainless Steel	102	64	4.1	6.6	12.3	217.6	42.8	811	208.43	3.89	15.51	30.75
Magnesium	152	76	6	6	18.6	662	87.2	185	102.31	1.81	22.10	10.62

For each alternative material selection for the I-cross beams, Table 3.4 specifies the minimum standard dimensions required for the I-beam cross-section in order to meet

the design criteria outlined above. In addition, Table 3.4 displays the factor of safety, the mid-span deflection, and the weight of the unit floor area corresponding to every material option for the I-cross beams.

The results presented in Table 1 reveal that the current weight of a baseline van floor can be reduced by as much as 69 or 66 percent when the steel I-cross beams are replaced, through an integrated design approach, by I cross-beams made of carbon-carbon composite or magnesium alloy, respectively. These results demonstrate the drastic reductions in structural weight that can be achieved through rational applications of lightweight materials in heavy vehicles that integrate the layout and geometric design with the material selection process. This conclusion is further supported by similar studies on three other alternative design concepts for the trailer floor, as follows:

Alternative 2: Sandwich panel consisting of top and bottom fiberglass faceplates and a core formed of transverse C-channel cross beams, as shown in Figure 3.11. Table 3.5 lists the minimum dimensions required for the C-channel beams for each alternative candidate material in order to meet the design criteria outlined above.
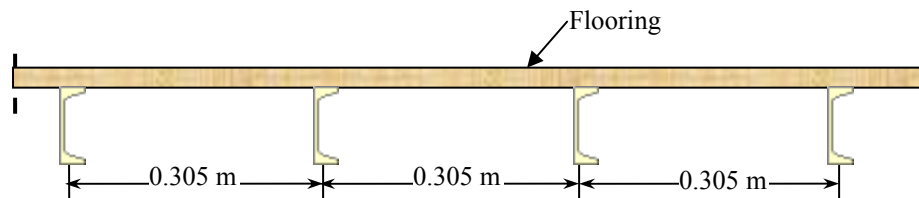
Figure 3.11 C-Channel Beam Floor.

TABLE 3.5 Alternative Material Solution for C-Channel Beam Floor.

MATERIAL CANDIDATE	SIZE				Section Properties			Ultimate Strength	Flexural Stress	Factor of Safety	Mid-span Deflection	Weight
	d	b_f	t_w	t_f	A	I_{xx}	S					
	mm	mm	mm	mm	cm²	cm⁴	cm³	MPa	MPa		mm	kg/m²
STEEL	127	44	4.8	8.2	12.71	311.8	49.16	550	181.46	3.03	10.05	32.71
Aluminum	152	83	5.3	8.9	22.11	890.7	114.9	240	77.66	3.09	10.41	19.67
EXTREN 525	254	70	13	13	46.77	3848	303	206	29.44	7.00	8.86	26.85
Carbon-Carbon	152	43	9.5	9.5	20.84	605.6	79.48	1096	112.25	9.76	7.65	10.80
Nitronic 19D Stainless Steel	127	44	4.8	8.2	12.71	311.8	49.16	714	181.46	3.93	10.20	32.19
Nitronic 60 Stainless Steel	127	44	4.8	8.2	12.71	311.8	49.16	1110	181.46	6.12	10.72	32.78
NItronic 30 Stainless Steel	127	44	4.8	8.2	12.71	311.8	49.16	811	181.46	4.47	10.83	31.77
Magnesium	152	83	5.3	8.9	22.11	890.7	114.9	185	77.66	2.38	16.80	12.62

Alternative 3: Sandwich panel built of ribbed fiberglass faceplates with a core consisting of hollow cross tubes of either rectangular or circular cross-section, as shown in Figure 3.12. Table 3.6 lists the minimum dimensions required for the tube core beams for each alternative candidate material in order to meet the design criteria outlined above.
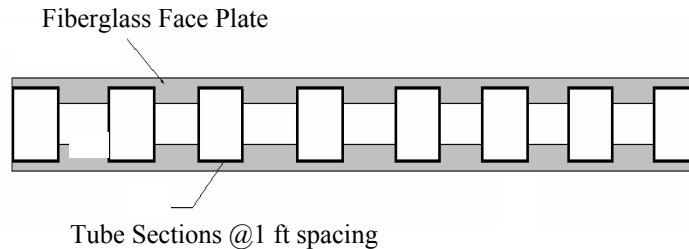
Fiberglass Face Plate

Tube Sections @1 ft spacing

Figure 3.12 Alternative Material Solution for Tube Core Floor.

TABLE 3.6 Alternative Material Solution for Tube Core Floor.

	SIZE				Section Properties			Ultimate Strength	Flexural Stress	Factor of Safety	Mid-span Deflection	Weight
	d	b_f	t_w	t_f	A	I_{xx}	S					
MATERIAL CANDIDATE	mm	mm	mm	mm	cm^2	cm^4	cm^3	MPa	MPa		mm	kg/m^2
STEEL	102	76	7.94	24.1	310.09	60.96	102	550	146.34	3.76	10.11	61.99
Aluminum	152	76	7.94	32.2	878.25	115.2	152	240	77.44	3.10	10.56	28.46
EXTREN 525	229	152	7.9	24.3	1039.3	125.5	229	206	71.07	2.90	32.81	34.12
Carbon-Carbon	165	51	6	56.5	605.62	79.48	165	1096	112.25	9.76	7.65	29.30
Nitronic 19D Stainless Steel	102	76	7.94	24.1	310.09	60.96	102	714	146.34	4.88	10.25	60.95
Nitronic 60 Stainless Steel	102	76	7.94	24.1	310.09	60.96	102	1110	146.34	7.58	11.86	62.07
NItronic 30 Stainless Steel	102	76	7.94	24.1	310.09	60.96	102	811	146.34	5.54	11.00	60.16
Magnesium	152	76	7.94	32.1	878.25	115.2	152	185	77.44	2.39	17.03	18.34

Alternative 4: Floor constructed from sandwich panel with a homogeneous, lightweight core. Table 3.7 lists the minimum dimensions required for the different faceplates made out of each alternative candidate material in order to meet the design criteria outlined above.

TABLE 3.7 Alternative Material Solution for Sandwich Structure Floor.

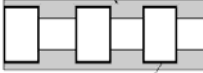|	SIZE		Section Properties			Ultimate Strength	Flexural Stress	Factor of Safety	Mid-span Deflection	Weight
	d	tf	A	Ixx	S					
CANDIDATE MATERIAL	mm	mm	cm^2/m	cm^4/m	cm^3/m	MPa	MPa		mm	kg/m^2
STEEL	102	1.6	16	832.32	160.68	550	185.07	2.97	12.55	25.09
Aluminum	152	1.6	16	1848.3	240.67	240	123.56	1.94	16.72	8.64
EXTREN 525	200	6	60	12000	1165	206	25.52	8.07	9.47	20.00
Carbon-Carbon	127	1.6	16	1290.3	200.67	1096	148.19	7.40	11.98	5.06
Nitronic 19D Stainless St.	102	1.6	16	832.32	160.68	714	185.07	3.86	12.74	24.70
Nitronic 30 Stainless St.	102	1.6	16	832.32	160.68	1110	185.07	6.00	14.73	25.16
Nitronic 60 Stainless St.	102	1.6	16	832.32	160.68	811	185.07	4.38	13.66	24.38
Magnesium	200	1.8	18	3600	356.79	185	83.35	2.22	13.85	6.26

The results of minimum weight, integrated design studies for all the above four alternative sandwich panel configurations of the trailer floor are summarized in Tables 3.4 to 3.7 for eight different material selections for the core of the panel. Both the maximum deflection and the minimum weight per unit area shown in Tables 3.4 to 3.7 for every design option considered here, meet the design criteria defined earlier in terms of the factor of safety and deflection limit.

The results displayed in Tables 3.4 to 3.7 indicate that, for any core material selection, the best design configuration for maximum weight savings is that of sandwich panels with light homogeneous core. On the other hand, the sandwich floor panel with core formed of cross C-channel beams may even increase the required weight of the floor for certain material choices for the core C-channels. However, this structural arrangement appears to provide higher stiffness than the other options compared here, for most of the material candidates listed in Tables 3.4 to 3.7. Carbon-carbon composites allow the largest weight reductions and the minimum deflections for any design configuration. Obviously, the benefits of using carbon-carbon cores are strongly dependent on the structural configuration of the floor. Additionally, the recent technologies being developed for producing low-cost carbon fibers would allow broader use of such material at a fraction of the current cost [15-18].

Every structural arrangement evaluated above could be further optimized by altering, for example, the spacing between cross beams in Figure 3.10, or the characteristics of the face sheets. However, the main objective of this study was to assess the predicted tradeoffs between weight savings and stiffness for alternate core material selections, and not the optimization of any one particular structural arrangement or another. The predicted energy savings enabled by the lightweight floor design and joining configurations of a typical van trailer are shown in Table 3.8 below. Although these numbers appear to be small for transporting one ton of cargo, they become enormously significant considering the thousands and thousands of freight that any given trailer is likely to haul during its life in service.

Since the operators of long haul heavy trailers usually load them to reach the gross vehicle weight (GVW) in order to maximize the efficiency of every transport, structural weight reductions would not necessarily result in lower fuel consumption of the truck in terms of "miles per gallon". Instead, the associated energy savings are best expressed in terms of fuel used by a heavy vehicle to transport one ton of freight over a certain distance, say 1,000 miles [gal/(kip*mile)]. The comparison illustrated in Table 3.8 indicates that the current weight of the floor in a typical van trailer can be reduced to half, or even less, if a sandwich panel design configuration and joining concept devised at WVU is utilized. The figures presented in Table 3.8 are based on the floor and chassis assembly of a 48-ft long van trailer, and a gross vehicle weight of 80 kips.

TABLE 3.8 - Energy Saving Through Lightweight Floor Design and Joining Concepts.

Alternative lightweight designs, based on sandwich panel configurations, for the floor of a typical heavy van trailer		Minimum Weight (lb)	Weight Saving (%)	Gallons of Fuel Used to Transport One Ton of Cargo Over 1000 Miles
Current configuration		6980	0%	5.82 (0.0%)
Fiberglass cross-beams		2802	60%	5.41 (7.0%)
Fibergalss Face-Plates, Core of Magnesium Hollow Tubes		3701	47%	5.49 (5.7%)
Fibergalss Face –Plates, Core of Magnesium C-Channels		3252	53%	5.45 (6.4%)
MMC Duralcan Face-Plates with lightweight core, such as Balsa		2964	57%	5.43 (6.7%)

CHAPTER FOUR

DESIGN AND ANALYSES OF BOLTED AND BONDED JOINTS

4.1   Modeling of Bolted Joints

Three_Dimensional Finite Element (3DFE) models have been developed for three different types of joining techniques in order to compare the behavior of the MMCs with other structural materials.

There models were developed for single and double lap bolted joint configurations, including load spreaders, or washers, inserted between the plates and the bold head or nut.   The main feature in such models is the explicit modeling of the contact interfaces between the jointed plates, between the load spreaders and joining plates, and between the bolt surface and the holes. Figure 4.1 illustrates the finite element mesh of a double lap joint.
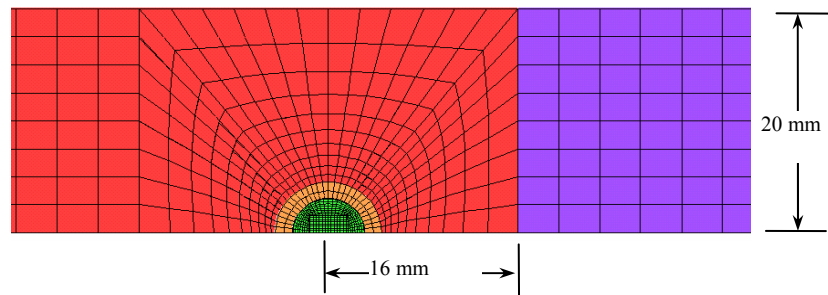

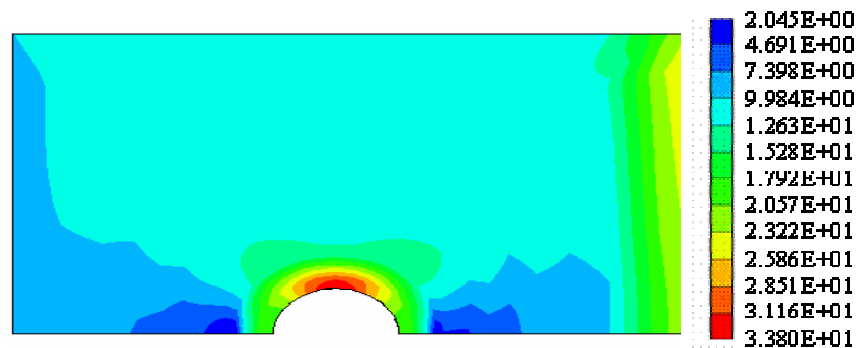Figure 4.1 Finite Element Model of the Double Lap Bolted Joint.

Figure 4.2 Von-Mises Stress Distribution around a Hole in a Double Lap Bolted Joint.

An axial tension load was applied on the model, and the resulting stress field around the bolt was determined and analyzed. As one could expect, the results of the finite element simulation confirm the presence of bending of the jointed plates in single lap joints, caused by the load eccentricity between the two plates. This bending effect significantly reduces the contact stresses between the bolt and the cylindrical hole surface. However, high contact stresses develop around the hole in the case of double lap joints, as illustrated in Figure 4.2

4.2   Parametric Study on Bolted Joints

Parametric analyses of the single and double lap joint have been conducted over a wide variety of design parameters such as the material properties of the jointed plates, the washers (load spreader) diameter, the clearance between the hole and the bolt, the diameter of the bolt, and its tightening pressure. The main findings of this parametric study can be summarized as follows:

a) Increasing the bolt tightening pressure from 0 to 30 kN resulted in 75% increases in the average effective stress around the hole, both for single and double- lap joints.
b) The Young's Modulus of the connected plates has an insignificant effect on the stress distributions around the hole. The strain levels around the hole however increase as the Young's Modulus decreases.
c) In single lap joints, the effective stress around the hole increases when the bolt diameter or the washer diameter increases. This effect is, most likely, due to the bending associated with the asymmetric loading of the joint.
d) Increasing the clearance between the bolt and the hole from 0.02 mm to 0.15 mm decreased the level of stresses around the hole by 65%.
e) In double lap joints with a 6 mm bolts, increasing the washer diameter from 8 to 12 mm decreased the contact stresses by 70%. Any further increase in the washer diameter has insignificant effect on the stresses around the hole.
f) In a double lap joint, increasing the bolt diameter from 5 to 6.5 mm resulted in a 30% increase in the maximum stress around the hole.

4.3   Failure Analyses of Bolted Joints

Failure analysis has been conducted for double lap bolted joints made of different materials such as steel, aluminum, aluminum with 30% silicon carbide reinforced, and aluminum with 55% silicon carbide reinforcement were assumed for the jointed plates.

Figure 4.3 depicts the effective stress distribution around the hole before the onset of failure. The results conform the expected drawbacks associated with the brittle failure of MMC materials. The MMC joint is predicted to fail in the "bearing" mode, where the rear surface of the hole that is in direct contact with the bolt is crushed without yielding. Moreover, the use of such MMC materials for the jointed plates may cost 12-14 folds more than equivalent aluminum joints, with no performance benefits.
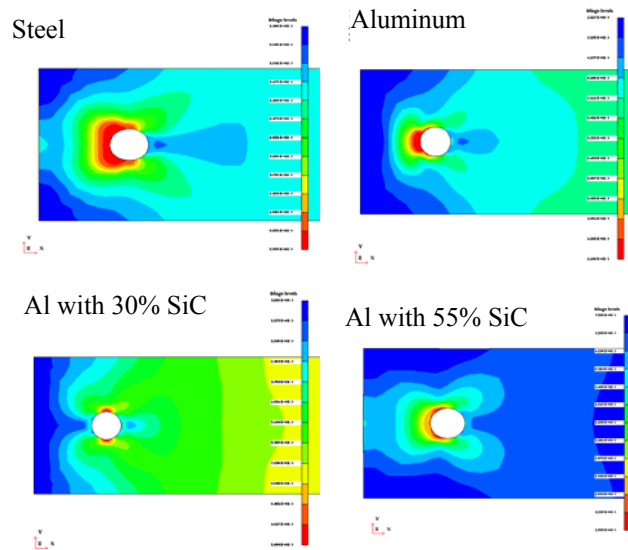
Figure 4.3 Stress Distribution Around Hole Before Failure.

Three dimensional finite element modeling was also used for failure simulation of double lap bolted joints made of "Duralcan" and "LANXIDE"Metal-Matrix Composite (MMC). Both materials are composed of aluminum matrix reinforced by Silicon Carbide particles. The 3DFE models were built to simulate bolted joint specimens of different geometric configuration that were experimentally tested under the effect of unixial tensile load as illustrated in Figure 4.4.
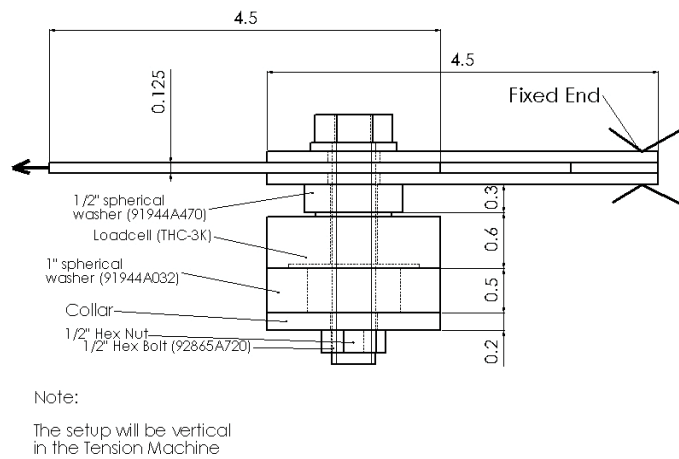
Figure 4.4 Testing Setup of Bolted Joint.

The material properties used in the 3D FE model for Duralcan and LANXIDE were experimentally measured on standard specimens that were tested according to ASTM

standards E8M and D-70. The tests results of material characterization of both materials are summarized in Table 4.1

TABLE 4.1 LANXIDE Vs. Duralcan Properties

	Lanxide 30% Sic		Duralcan 20 % Sic	
	Measured	Published	Measured	Published
Young's Modulus	15.45 Msi	15.97 Msi	17.73 Msi	14.6 Msi
Ultimate Strength	15.6 ksi	32.6 Ksi	25.39 Ksi	42.0 Ksi

Table 4.2 presents the specimen configurations as well as a comparison between the measured failure load and that predicted using 3D FE model. An excellent agreement can be observed between theoretical and experimental results for Duralcan specimens. However, larger deviation is found between the 3DFE predicted failure load and the experimentally measured ones. These differences could be attributed to the inconsistency in the material properties of LAXIDE properties any invisible defects that may be formed in the specimens during the machining process what was extremely difficult.

TABLE 4.2 Test and 3DFE Models Results for Duralcan and LANXIDE Bolted Joints.

Specimen	e (in.)	w (in.)	Duralcan Failure Load (Lb)			LANXIDE Failure Load (lb)			Failure Mode
			Measured	3D FE	Difference	Measured	3D FE	Difference	
Specimen 1	2.5	2.0	3561	3776	6%	2277	1350	-41%	Net Section
Specimen 2	1.5	2.0	2516	3500	39%	1740	1350	-22%	Net Section
Specimen 3	0.6	2.0	1294	1348	4%	516	700	36%	Shear pullout
Specimen 4	2.5	1.5	2139	2360	10%	2121	1300	-39%	Net Section
Specimen 5	0.6	1.5	1353	1264	-7%	490	674	38%	Shear pullout

Net Section   Shear Pullout
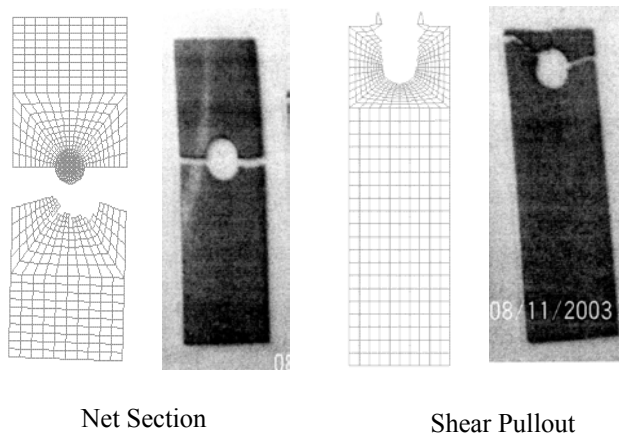
Figure 4.5 Failure Modes of MMC Joints.

The accuracy of the 3DFE model developed for MMC bolted jointed was not only validated by the agreement between the 3DFE-calculated failure load and the experimentally measured one, but also by predicting the same mode as illustrated in Figure 3.5

4.4   Bonded Joints

Bonded single and double lap joint have also been modeled for extensive parametric over a wide range of adhesive and adherent material properties as well as various material configurations. The main conclusions of this study can be summarized as:

a)   As the thickness of the adhesive increases, the shear stress becomes uniform along the overlap length. The maximum shear stress decreases as the adhesive thickness increases.
b)   The shear stress at the free edge in the adhesive is reduced by 60% due to the tapering in the outer adherent at 45º.
c)   The spew fillet reduces the shear stress at the free edge in the adhesive by 65%.

Modeling of friction stir welding is focused on the predictions of energy balance, conversion and exchange between the tool piece and the jointed plates.

CHAPTER FIVE

EXPERIMENTAL CHARACTERIZATION OF MMC MATERIALS
AND BOLTED JOINTS

5.1   Introduction

Different versions of Aluminum/Silicon Carbide MMC material marketed under the name "LAXIDE" trademark have been experimentally tested for possible applications in heavy vehicle structures. The material characterization were carried according to the relevant ASTM Standards and ranged from micro-structural evaluation to hardness, thermal, elastic and strength properties. The characterization testing also included the material testing of another type of Aluminum/Silicon Carbide MMC material marketed under the name "Duralcan" trademark. The tests results indicated that the brittleness of this MMC material seriously degraded its design strength, despite the fact that its stiffness is more than twice that of aluminum, and its Vickers hardness is higher than aluminum (by 52% for 30% SiC reinforcement and by 37% for 45% Sic reinforcement). Due to the low conductivity of SiC particles, the coefficient of thermal expansion for this MMC material was found to be lower than that of aluminum. Such inconsistent quality of the LANXIDE material and the difficulty encountered in its machining turn out to be a major problem to any potential use in heavy vehicles. The sensitivity of the MMC material to processing conditions during manufacturing requires independent validation for the material properties, which is inconvenient for potential industrial application.

5.2   Testing of Bolted Joints

A test matrix of 36 Aluminum and MMC specimen has been planned and carried out for experimental characterization of double lap bolted joints of different geometric configurations. Figure 4.1 illustrates a schematic drawing of the experimental setup used for testing double-lap bolted joints.
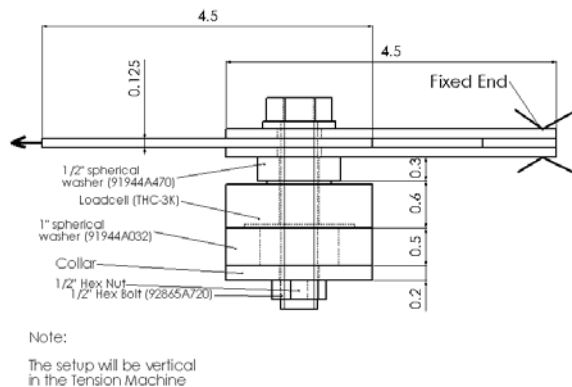

Figure 5.1 Testing setup of Bolted Joint.

The test results indicate that the failure mode as well as the failure load in bolted joints depends up two ratios:

1. Width of the specimen to hole diameter (w/d).
2. Distance from joint edge to hole center to hole diameter (e/d).

The test matrix included specimens with "e/d" ratio varying from 1.2 to 5, for three different "w/d" ratios: 3, 4, and 8. The bolted joints were tested at clamping forces of 50lbs (finger tight conditions),1000lbs and 2000 lbs.   Figure 4.2 illustrates the dimensions of the specimens used for testing of bolted joints.
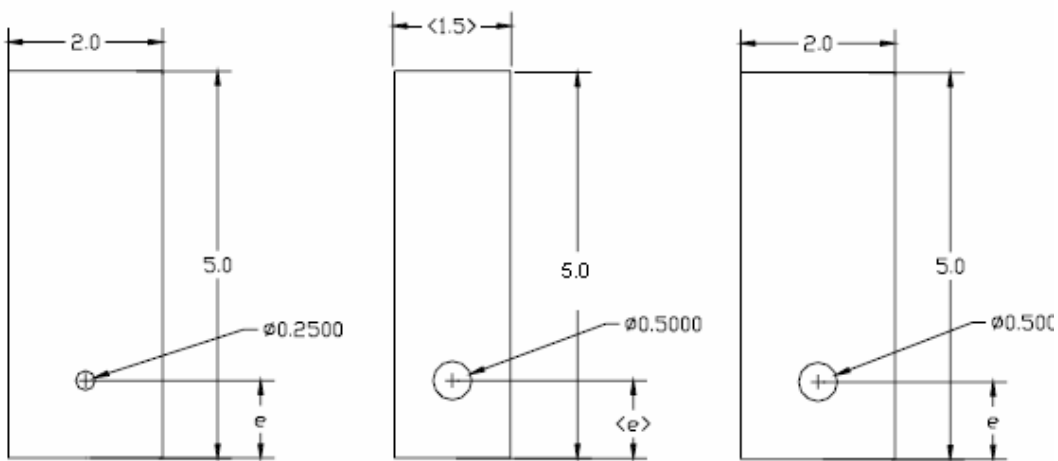
Figure 5.2 Dimensions of Specimen Used in the Bolted Joint Testing.

Al/Sic MMC material with 45% volume fraction specimens were cut from cast blocks of material obtained from the manufacturers. The preparation of joint specimens, when cut from conventional carbide blades was hindered by many mechanical problems. Specially manufactured diamond tipped tools has to be used eventually, in order to overcome these difficulties. The 20% specimens were however machined by using the electrical discharge machine, which was used to first cut slices from the MMC brick and these slices were further machined into the required shape. On the 45% SiC specimen, large surface defects in the specimens could be observed after the machining. The defects were seen in 13 out of 36 specimens that were prepared for testing purposes as shown in Figure 5.3. A microscopic analysis was performed at the regions of defect and it was clearly visible that these regions did not contain any SiC particles and this can be attributed as a processing defect as can be seen in Figure 5.4. This is confirmed by performing a hardness tests in the SiC rich and SiC poor regions.
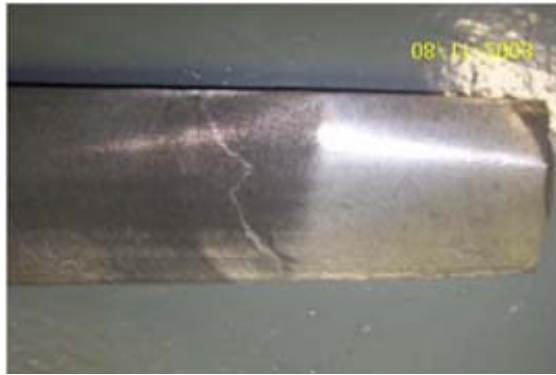
(a) MMC Specimen with Defect in Transverse Direction

(b) MMC Specimen with Defect in Longitudinal Direction

Figure 5.3 Manufacturing Defects in LANXIDE MMC Specimens.
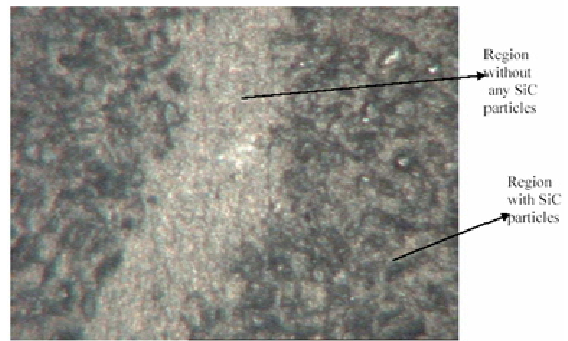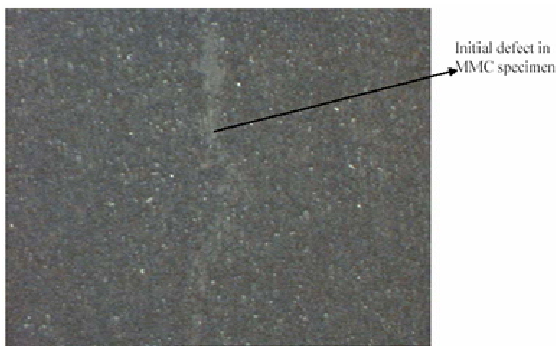
Figure 5.4 Microscopic Views of LANXIDE MMC Specimens with
Vickers Indentation in Regions with Defects

5.3   Experimental Results and Discussion

5.3.1   Specimens with 45% Reinforcement

Typical load displacement curves of the double-lap joints made of 45% MMC are presented in Figures 5.5 and 5.6. These curves have been generated under displacement controlled loading for a clamping force value of 50 lbs (finger tight conditions). The results show that the load rises steadily to an ultimate value at which the joint fails without any yielding. One may notice that for higher values of the e/d ratio, the ultimate failure load increases with the specimen still failing in the net-section mode, but without any yielding.
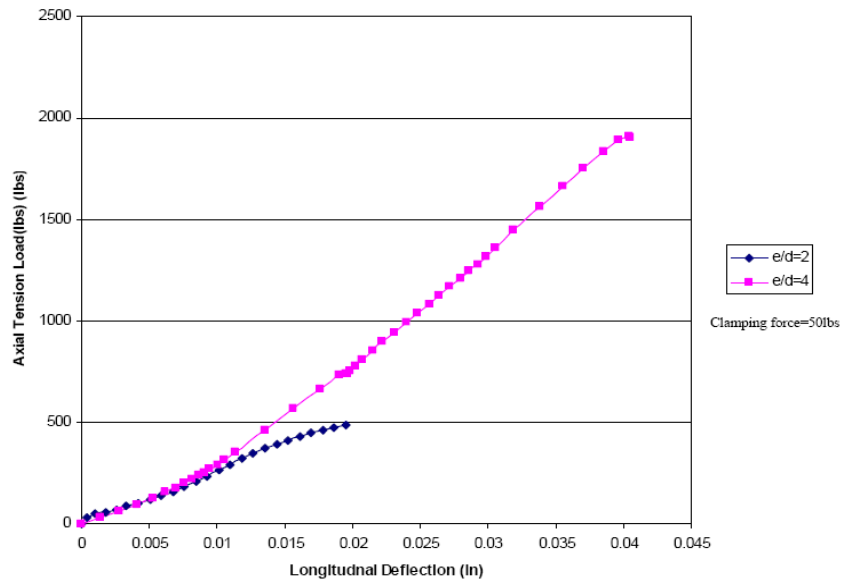
Figure 5.5 Load-Displacement Relationship of Joint Specimens with 'w/d" Ratio of 3
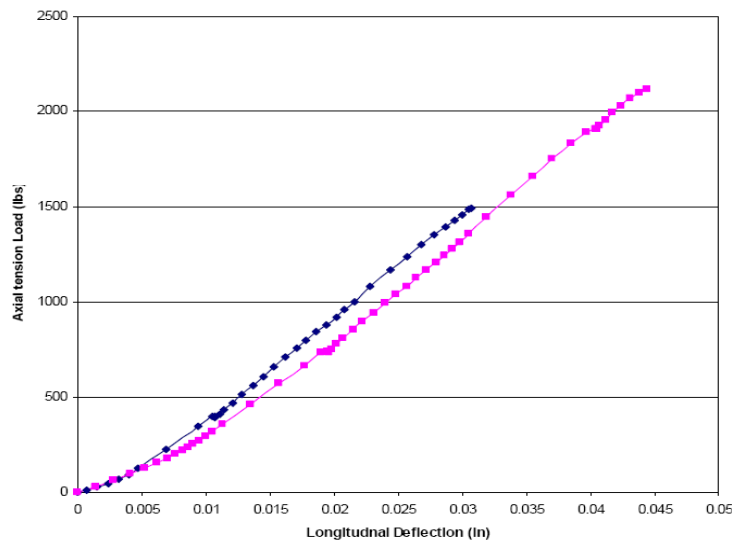
Figure 5.6 Load-Displacement Relationship of Joint Specimens with "w/d" Ratio of 4

34

It was also seen that the slip load increases with the increase in the clamping force. The slip load is defined as the load at which the friction between the plates becomes negligible and slipping occurs. Thus, no slippage is seen under finger tight conditions as there is no frictional support in this case. Most of the slip occurred between 40 and 80 percent of the ultimate strength of the material.

The effect of the clamping force magnitude on the tensile strength of bolted joints is an important parameter in bolted joint design. The ultimate strength of bolted connections increases when the clamping force increases as shown in Figure 5.7 and Table 5.1. This increased load bearing capacity of the joint can be attributed to the increased friction between the joined plates by the bolts which enables them to spread the high stresses around the hole over a larger area and thus reduce the bearing contact stresses between the bolt and the hole. However, it is noticed that the clamping pressure does not change the mechanism of failure for MMCs.
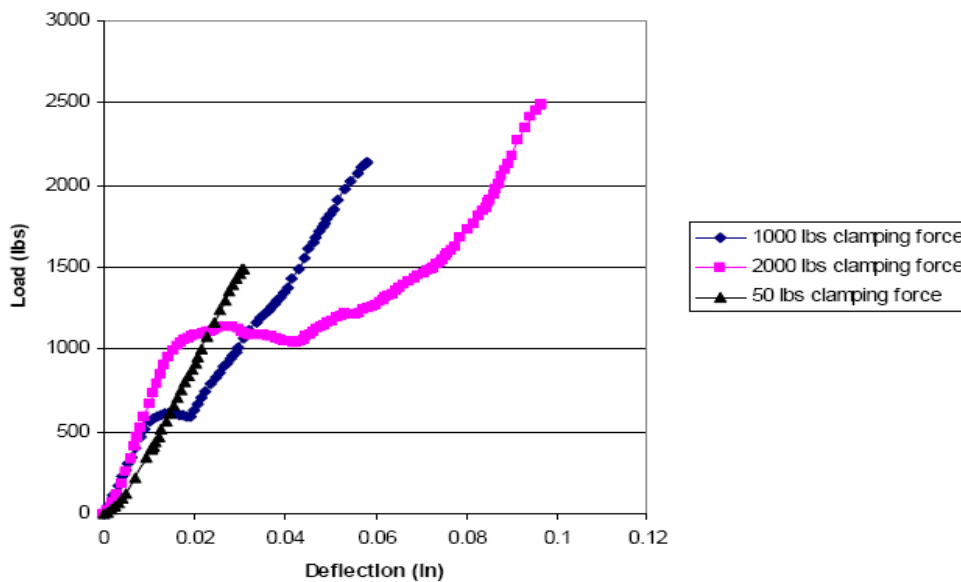
Figure 5.7 MMC Joint Specimen under Different Clamping Conditions.
(e/d=2 and w/d=4)

It is seen that initially, the clamping force remains a constant. But with the increase in the axial load, the clamping force also increases, though only to a small extent to about 60 lbs from finger tight conditions.

Tables 5.1 to 5.3 illustrate the experimental values of the ultimate load for the double lap-joint of MMC material. It is seen that this load is much lower than the theoretical loads calculated from the European standards. For specimen having e/d=1.2, shear edge pullout is the seen kind of failure seen. For all other values of e/d ratio, net-section failure is seen.

TABLE 5.1 Failure loads of 45% SiC joints for w/d ratio = 4.0

e (in)	d (in)	e/d ratio	Initial clamping force (lb)	Failure Load (lb)	Failure mode
0.6	0.5	1.2	50	516	Shear pullout
0.6	0.5	1.2	1000	916.42	Shear pullout
0.6	0.5	1.2	2000	1597.41	Shear pullout
1	0.5	2	50	1493.63	Net section
1	0.5	2	1000	2144.51	Net section
1	0.5	2	2000	2494.91	Net section
1.5	0.5	3	50	1739.57	Net section
1.5	0.5	3	1000	2095.06	Net section
1.5	0.5	3	2000	2949.42	Net section
2	0.5	4	50	2120.65	Net section
2.5	0.5	5	50	2277.19	Net section

TABLE 5.2 Failure loads of 45% SiC joints for w/d ratio = 3.0

e (in)	d (in)	e/d ratio	Initial clamping force (lb)	Failure Load (lb)	Failure mode
0.6	0.5	1.2	50	489.54	Shear pullout
1	0.5	2	50	1157.02	Net section
1.5	0.5	3	50	1661.53	Net section
2	0.5	4	50	1998.75	Net section
2.5	0.5	5	50	2120.56	Net section

TABLE 5.3 Failure loads of 45% SiC joints for w/d ratio = 8.0

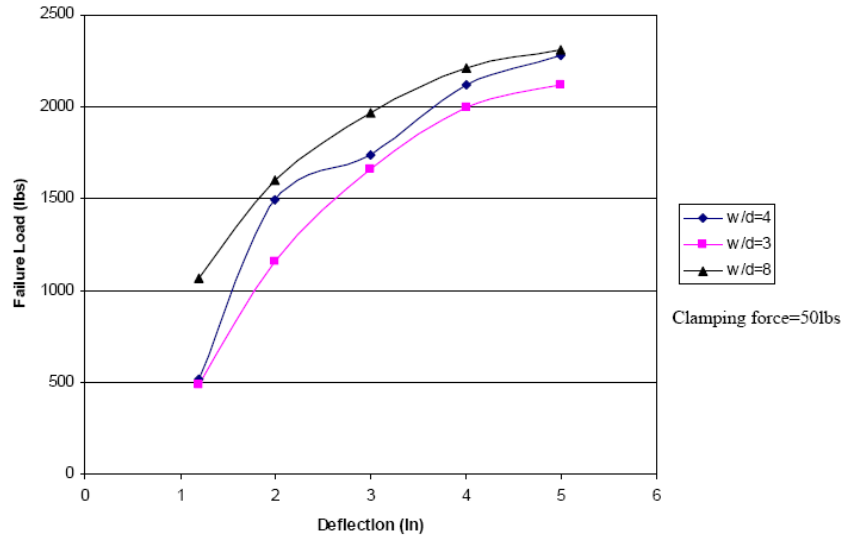| e (in)	d (in)	e/d ratio	Initial clamping force (lb)	Failure Load (lb)	Failure mode
0.6	0.5	1.2	50	1066.75	Shear pullout
1	0.5	2	50	1604	Net section
1.5	0.5	3	50	1967.69	Net section
2	0.5	4	50	2210.78	Net section
2.5	0.5	5	50	2312	Net section

Figure 5.8 Variation of The Failure Load With the "e/d" Ratio

From the values of the failure loads, it is clear that an increase in the "w/d" ratio results in an increase in the failure load. It is to be noted that none of the joints failed under bearing mode, even for higher values of "w/d" ratio. This is due to the reduced ductility of the MMC material, which induces net-section failure rather than bearing failure. The maximum net section failure strength was obtained at "w/d"= 8.0, beyond which the increase in maximum failure load with the "w/d" ratio was minimal. Figure 5.8 illustrates that the ultimate load increases with the increase in the "e/d" ratio for all values of "w/d" ratio.

Table 5.4 captures a summary of the various failure modes observed in these tests, as function of the "w/d" and "e/d" ratios of the test specimens. Figure 5.9 shows photos of the MMC joint specimens that failed either in the "net-section" or "bearing" modes of failure.

TABLE 5.4 Variation of Failure Mode with Specimen Geometry.

e/d	w/d ratio		
	3	4	8
1.2	Shear out	Shear out	Shear out
2	Net-Section	Bearing	Bearing
3	Net-Section	Bearing	Bearing
4	Net-Section	Bearing	Bearing
5	Net-Section	Bearing	Bearing
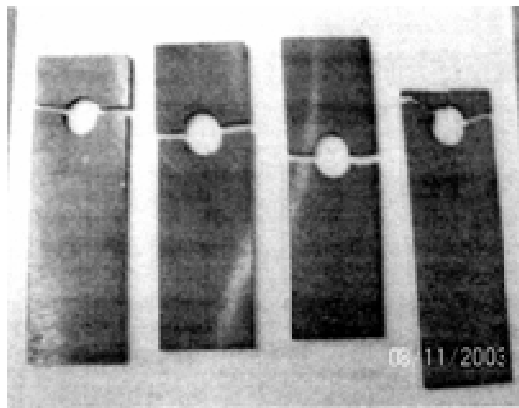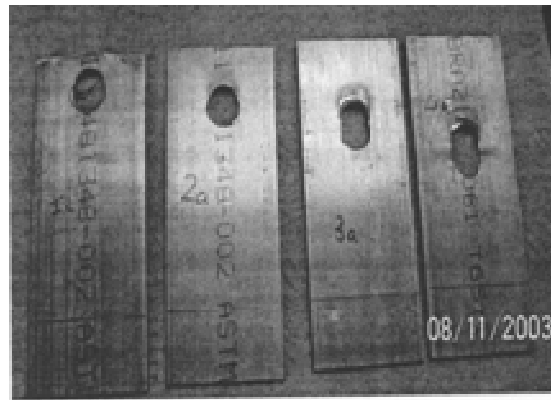
| (a) Net-Section failure | (b) Bearing failure |
| (w/d=3) | (w/d=4) |

Figure 5.9 Failure Modes

5.3.2   Specimen with 20% Reinforcement

A smaller number of specimen made of 20% SiC reinforcement were tested for the sake of comparison. Table 5.4 lists the failure load of the joints and their modes of failure.

TABLE 5.4 Failure Loads of 20% SiC Joints.

e (in)	e/d	w(in)	Initial clamping force (lb)	Failure Load (lb)	Failure mode
2.5	5	2	50	3560.51	Net section
1.5	3	2	50	2516.0	Net section
0.6	1.2	2	50	1293.94	Shear pullout
2.5	5	1.5	50	2138.78	Net section
0.6	1.2	1.5	50	1352.51	Shear pullout

It is clear that the joints made of 20% SiC proved to be stronger than the joints having 45% SiC. This is caused by the defects in the 45%-Al/SiC MMC material discussed earlier. These surface defects can substantially reduce the strength of the joint by acting as centers of crack initiation. The failure modes seen in the 20% samples are the same as those seen earlier. As a general trend, it is seen that the clamping force increases with the increase in the axial tensile load. However, the rate of increase of the clamping force is higher for specimens having low "e/d" ratios. The variation of the clamping force with the axial load is shown in Figures 5.10 and 5.11.
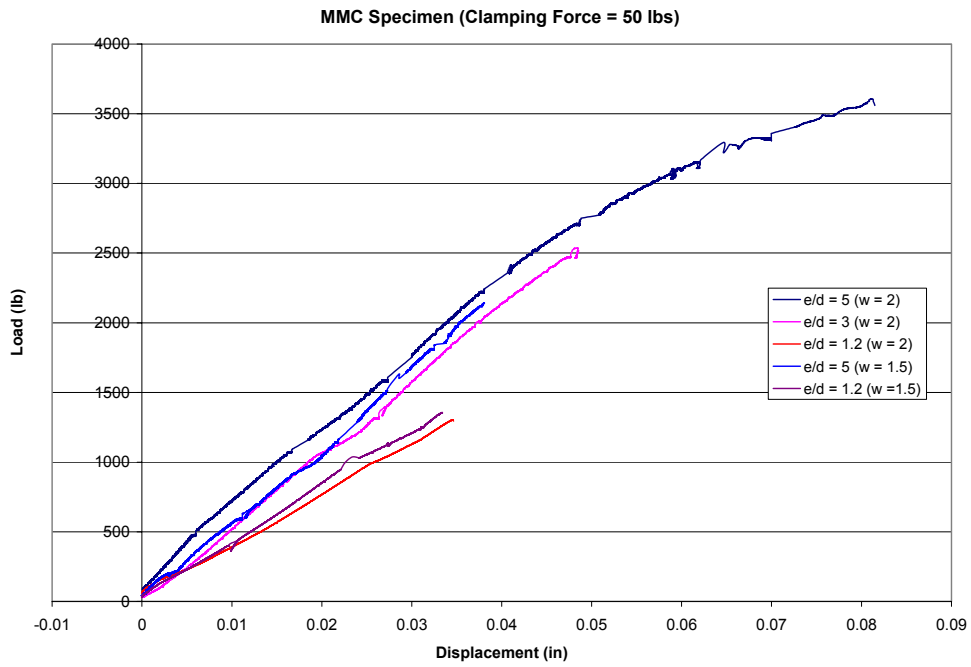
Figure 5.10 Load-Displacement Relation for 20% SiC Bolted Joint Specimens
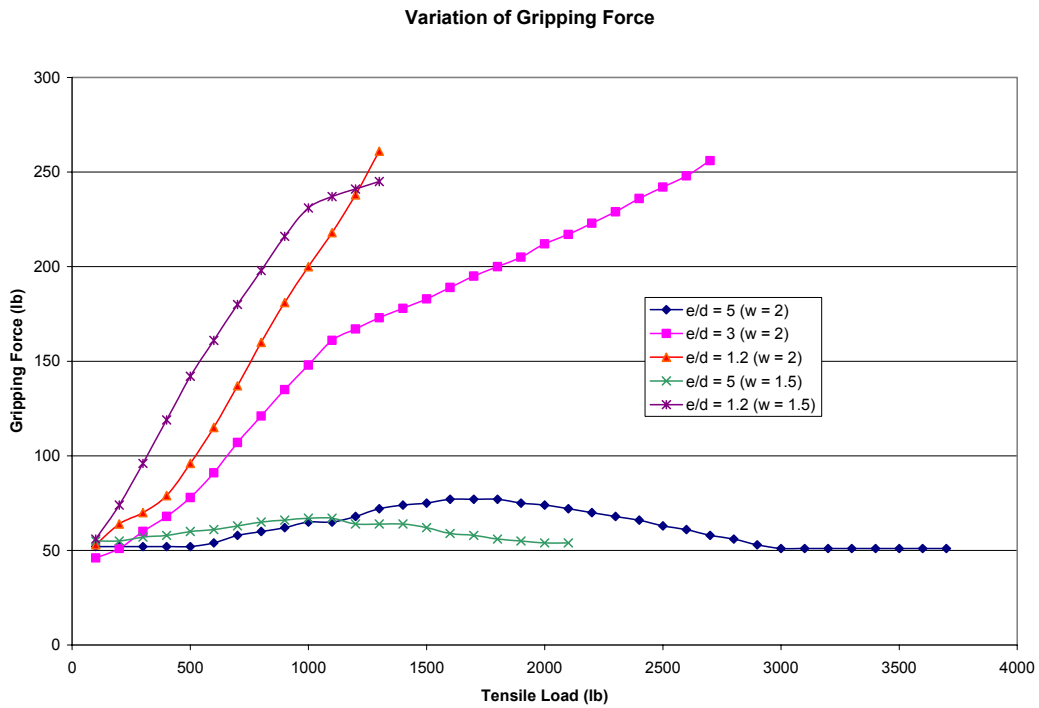

Figure 5.11 Variation of Clamping Load with Axial Tensile Load.

5.4   Conclusion

From the present work of characterizing the bolted joints, following conclusions can be drawn:

1. Double-lap joints made of MMC material fail by net-section failure rather than the bearing mode of failure which is common for aluminum joints. Even for such a large w/d ratio as w/d=8.0, when the material was expected to fail through bearing, it actually failed through net-section failure and edge shear pull out.

2. The net section failure load increases with increasing the values of e/d and w/d until it becomes almost a constant. The highest values of the net section failure load was observed at e/d=5.0 and w/d= 8.0 configuration of the double-lap joint.

3. It is noticed that that when the clamping force is increased to 1000 or 2000 lbs the net section failure load also increases, which proves again the effect of lateral clamping pressure on failure strength of a double-lap joint.

4. Slip between the jointed plates is noticeable at clamping force levels larger than 1000 lbs, when the friction force affects the failure strength of the bolted joints.

CHAPTER SIX

PROTOTYPING OF SCALED MODEL OF TRAILER

6.1   Scale Trailer Model

A 1:4 scale model of a truck cargo haul was designed and fabricated to understand the joining concepts and requirements to successfully connect composite materials as an alternative to bolting methods as shown in Figure 6.1. The use of revolutionary composite materials in the design serves to decrease the comparative weight of the model to the existing trailer design.

The process of fabricating the model was a method to test the feasibility of the researched joining methods. The process provided a means to analyze the designs first hand in fabrication, construction, and structural integrity.

The construction of the model was the culmination of a four month period of design and fabrication. It started from the selection of the materials to be used through construction of fitting, processing, and joining parts to end with a 1:4 scale model of the cargo haul. The model replicates a full scale trailer and will aide in analyzing the effects of joining and bonding of composite materials. The model will be used for further analysis through finite element modeling and structural testing.

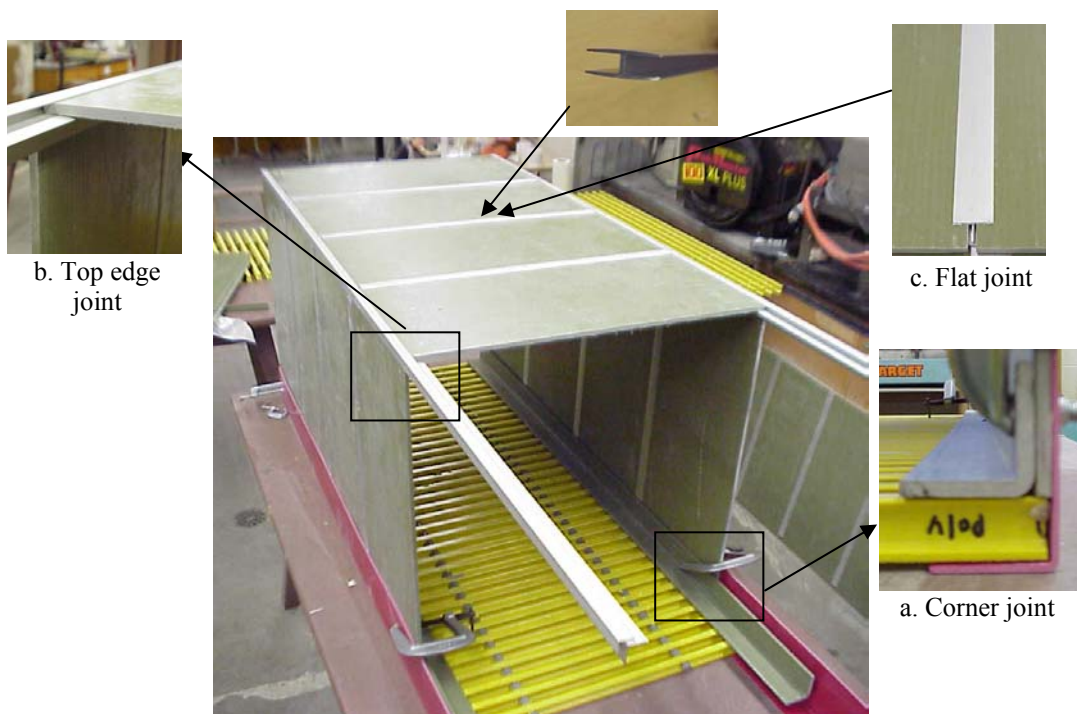b. Top edge joint

c. Flat joint

a. Corner joint

Figure 6.1 Inside View of the Van Trailer Model.

The fabrication of the model involved detailed design concepts to physically attain strong joints and bonds. The model construction involved tailoring fiberglass composite panels, I-beams, and angles to fit design specifications. A combination of aluminum and fiberglass was used to replicate the final design of high performance fiber reinforced polymer composites and metal matrix composites. The final design plan is to use revolutionary composite materials and metal matrix composites to provide low weight and high strength properties.

The building of the model was done in steps to ensure the feasibility of design concepts. The first phase was to complete the rear section of the model. This provided ideas and changes for the trailer design on a whole. The following standard parts were used in the construction of the model:

- ¼" thick fiberglass panels
- 1" Standard fiberglass I-beams
- Fiberglass rods
- Fiberglass angles
- Anodized aluminum H-channels
- Anodized aluminum J-channels
- Anodized aluminum U-channels
- Anodized aluminum cornering channels

Tailoring the parts involved cutting fiberglass panels and I-beams by specialized carbide tipped tools. The fiberglass panels are used as the top and side material of the trailer and also as a floor covering. I-beams are the main constituent of the floor material; they will accept and withstand the loads occurring on the truck bed floor. The I-beam sections are reinforced by "bearing bars" which run perpendicular to and through the web of each I-beam. The fiberglass bearing bars are important to provide connections to the bogey, landing gear, and kingpin on the underside of the trailer. Aluminum H-channels and edge corners were cut and manufactured to provide connections between adjacent side panels and a connection of the side panels to the top panel. The H-channels are anodized aluminum with ¼" openings to accept the thickness of the side panels. The H-channels had to be cut to the proper height and trimmed to allow proper spacing with the corner edge trim. The U-channels and J-channels are used as trim for the rear door of the trailer.

Bonding of the side panels has been done to secure the H-channel joint. The sides of the trailer have been segmented to allow flexibility to absorb forces experienced through loading. The bonding process requires thoroughly cleaning the aluminum channels and roughing the fiberglass panels with sandpaper. *Araldite 2021* toughened methacrylate adhesive has been used to bond the fiberglass to metal. *Araldite 2021* provides a bond that will fill voids between the mating parts and also has elastic characteristics in its cured state.

6.2　Modular Design

The model was designed and constructed to be modular and segmented. The model has three middle segments that are removable and replaceable. The model can therefore expand or contract in length from 9' to 12' in 1 foot increments with respect to the 1:4 scale model dimensions. This is an added feature that would eliminate trailer weight when a full cargo load is not being transported. Also this feature allows for replacement of damaged sections of a trailer and not the whole trailer.

In conclusion, the model provides a physical representation to determine the practicality of joining concepts, floor design, side and top panel configuration and bonding techniques. It has significantly activated more ideas to develop the most effective methods for joining and part design. There are many more options and design concepts that can make the model lighter, stronger, efficient in production and assembly. The steps taken so far have equipped us with the ideas and confidence to improve on the current design.

CHAPTER SEVEN

DURABILITY PREDICTIONS OF PARTICULATE
METAL MATRIX COMPOSITES

A new task has been initiated in the second year of this project to develop a predictive model for the effects of intrinsic and/or externally induced multi-scale damage on the residual service life of fiber and particulate-reinforced composite materials in critical components of heavy vehicle structures. The model relies on the periodic microstructure of such materials and leverages earlier research performed at West Virginia University in the area of Continuum Damage Mechanics (CDM) of fiber-reinforced Polymer Matrix Composites (PMC). The major contribution of those efforts so far is the development of a CDM model formulated in terms of parameters that can be measured easily from standard ASTM tests of single lamina coupon specimens and utilized for predicting the non-linear response of macro-scale laminates in the presence of damage [27, 28].

The main objective of the current task is to develop an analytical model for analyzing the behavior of damaged particulate-reinforced metal matrix composites (PMMC) subjected to monotonic loading, by expanding and modifying the prior work on fiber-reinforced composites. This approach allows cost-effective quantification and analysis of material property loss associated with damage initiation and accumulation in structural components made of PMMC or other composite materials. To achieve this goal, the model will be developed as a user-defined input to a commercial finite-element software package, such as ANSYS. A survey of pertinent literature dealing with the onset of localized micro-scale crack initiation and growth in extruded PMMC materials [29, 30] reveals that damage initiates at the micro-scale from clustering of the reinforcement particulate in certain regions throughout the PMMC material [31]. Consequently, this task is currently focused on the implementation of periodic microstructure techniques, along with CDM modeling, in order to describe the constitutive behavior of PMMC materials subject to monotonic loading through the analysis of clustering regions. Periodic microstructure techniques are used to determine the effective properties of the PMMC material with homogenized clustering regions, as depicted in Figure 6.1.
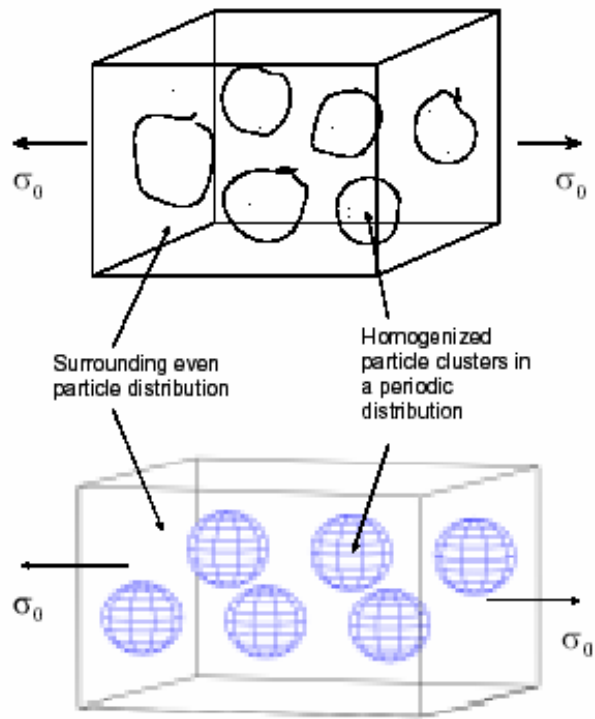
Figure 7.1 Homogenization of Particle Clusters in MMC Model.

CHAPTER EIGHT

CONCLUSIONS

8.1 Conclusions

- Alternative structural arrangements for the floor of a heavy van trailer have been devised and analyzed, leading to the conclusion that sandwich panels allow minimum weight designs for a variety of core configurations.

- Alternative material selections have been considered for the structural floor of a heavy van trailer, leading to the conclusion that carbon-carbon composites enable the greatest weight savings, depending on the specific floor design configuration.

- Alternative fastener-less joining methods between sandwich panels in various sections of a typical van trailer structure have been devised and evaluated, both through theoretical modeling and actual prototyping.

- Double-lap-bolted joints made of different MMC materials have been evaluated both through standard ASTM tests and failure simulations based on finite-element analysis, leading to the conclusion that such joints are likely to fail early in the bearing mode, because of the brittle behavior of MMC materials.

8.2 Directions for Future Research

- Develop and validate integrated, minimum-weight design concepts of full-scale structural assemblies for van trailers, based on sandwich panels with optimized face sheet and core configurations.

- Build a full-scale baseline prototype of a lightweight van trailer for extensive instrumentation and testing in realistic operation scenarios, as well as for showcasing the new concepts to producers and operators of heavy vehicles.

- Establish a knowledgebase for reliable durability predictions in terms of either fatigue life or damage tolerance of composite materials, for decision support in both the design and repair of structural components in heavy vehicle systems.

REFERENCES

1. "Research and Development Plan for High Strength /Weight Reduction Materials", Report on Workshop held at the National Transportation Research Center in Knoxville, Tennessee, April 24-25, 2002, DOE Report HSWR-001, September 2002.

2. "Requirements for Trailer Manufacturers", legislation and regulations established by the National Highway Traffic Safety Administration (NHTSA).

3. "Advanced Materials by Design", New Structural Materials Technologies, U.S. Congress, Office of Technology Assessment, Library of Congress Catalog Card Number 87-619860, June 1988.

4. "Metal Matrix Composites, A Technology Base Enhancement Program Project", Technical Report prepared by BDM Federal, Inc., for the North American Defense Industrial Base Organization (NADIBO), August 30, 1993.

5. Related Patents issued by the United States Patent Office:
    - "Coining Offset into Edge of Composite Plate Members for Forming Trailer Doors and Walls", Patent No. 5,938,274, Aug. 17, 1999.
    - "Composite Joint Configuration", Patent No. 6,412,854 B2, July 2, 2002
    - "Composite Joint Configuration", Patent No. 5,860,693, Jan. 19, 1999
    - "Composite Joint Configuration", Patent No. 6,220,651 B1, April 24, 2001
    - "Logistics at Composite Panel Vertical Joints", Patent No. 5,997,076, Dec. 7, 99
    - "Composite Cover for Transport Refrigeration Unit", Patent No. 5,338,424, Feb. 14, 1995
    - "Method of Punching a Composite Plate", Patent No. 6,266, 865 B1, July 31, 01.
    - "Composite Trailer Sidewall", Patent No. 4,958,472, Sep. 25, 1990.
    - "Intermodal Container Including Double Lap Shear Joints", Patent No. 5,741,042, April 21, 1998.
    - "Composite Floor", Patent No. 5,772,276, June 30, 1998
    - "Composite Wood Flooring", Patent No. 6,183,824 B1, Feb. 6, 2001
    - "Composite Trailer and Van Type Container Assembly Using Bi-Metal Materials", Patent No. 5,655,792, Aug. 12, 1997.

6. "Opportunities for Low Cost Titanium in Reduced Fuel Consumption, Improved Emissions, and Enhanced Durability of Heavy-Duty Vehicles", a study performed

by EHKTechnologies for the Oak Ridge National Laboratory, ORNL/Sub/4000013062/1, July 2002.

7. http://www.truckline.com/infocenter/opics/tech/011000_aerodynamics_attach.html

8. "Intercity Bus Weight Reduction Program", Phase 1, study report prepared for the Transportation Development Centre, Transport Canada, by Martec Ltd., Prevost Car, and Virtual Prototyping Technologies, TP 13560E, January 2000.

9. "Practical Economic Solution to Weight Reduction and Increased Performance in Diesel Engines", Louckes, T.N. (SinterCast Inc.), presented at the International Truck and Bus Meeting and Exposition, Nov. 18-21, 1991, Chicago, SAE Technical Paper Series, 1991, 912711.

10. "Composite Driveshafts: Technology and Experience" Leslie, James at al., in "Advanced Composite Products and Technology", SAE Special Publications, 1203, Oct., Issues in Commercial Vehicle Powertrain Design and Development, 1996, pp. 43-52, presented at the 1996 International Truck and Bus Meeting & Exposition, Oct. 14-16, 1996, Detroit, MI.

11. "Paying Off", Leavitt, Wendy Source DES, Diesel Equipment Superintendent , 73, 11, Nov. 1995, pp. 71-73.

12. "Metal Foams – A Design Guide", Michael F. Ashby et al., Butterworth-Heinemann, 2000, ISBN 0-7506-7219-6.

13. "Ultra -Lightweight Aluminum Foam Materials for Automotive Applications", Claar T. Dennis et al., International Journal of Powder Metallurgy, Princeton, New Jersey, 36, 6, September 2000, 10 pp. Published by the American Powder Metallurgy Institute, ISSN: 0888-7462 CODEN: IPMTEA.

14. "Selection of Engineering Materials", by Gladius Lewis, Prentice-Hall, Inc., 1990.

15. C.F. Leiteen, W.L. Griffith, and A.L. Compere (2002). Low-Cost Carbon Fibers from Renewable Resources. 2002 Annual Progress Report on Automotive Lightweighting Materials, U.S. Department of Energy, Washington, D.C., pp. 115-119.

16. H. Dasarathy, C.L. Leon, S. Smith, and B. Hansen (2002). Low-Cost Carbon Fiber Development Program. 2002 Annual Progress Report on Automotive Lightweighting Materials, U.S. Department of Energy, Washington, D.C., pp. 121-132.

17.   D.G. Baird, A.A. Ogale, J.E. McGrath, D.D. Edie (2002). Low-Cost Carbon Fiber for Automotive Composite Materials. 2002 Annual Progress Report on Automotive Lightweighting Materials, U.S. Department of Energy, Washington, D.C., pp. 133-136.

18.   F.L. Paulauskas (2002). Microwave Assisted Manufacturing of Carbon Fibers. 2002 Annual Progress Report on Automotive Lightweighting Materials, U.S. Department of Energy, Washington, D.C., pp. 137-142.

19.   C.F. Leiteen, W.L. Griffith, and A.L. Compere (2002). Low-Cost Carbon Fibers from Renewable Resources. 2002 Annual Progress Report on Automotive Lightweighting Materials, U.S. Department of Energy, Washington, D.C., pp. 115-119.

20.   H. Dasarathy, C.L. Leon, S. Smith, and B. Hansen (2002). Low-Cost Carbon Fiber Development Program. 2002 Annual Progress Report on Automotive Lightweighting Materials, U.S. Department of Energy, Washington, D.C., pp. 121-132.

21.   D.G. Baird, A.A. Ogale, J.E. McGrath, D.D. Edie (2002). Low-Cost Carbon Fiber for Automotive Composite Materials. 2002 Annual Progress Report on Automotive Lightweighting Materials, U.S. Department of Energy, Washington, D.C., pp. 133-136.

22.   F.L. Paulauskas (2002). Microwave Assisted Manufacturing of Carbon Fibers. 2002 Annual Progress Report on Automotive Lightweighting Materials, U.S. Department of Energy, Washington, D.C., pp. 137-142.

23.   J.R. Vinson (1999). The Behavior of Sandwich Structures of Isotropic and Composite Materials. Technomic Publishing Company, Inc. Lancaster, Pennsylvania.

24.   I. Kuch, F. Henning (2000). Thermoplastic Sandwich Structures with High Content of Recycled Material – An Innovative One-Step Technology. 21st SAMPE Europe International Conference, Paris, France, April 18-20, 2000.

25.   S.E. Mouring, R.P. Reichard (2001). Fabrication of a Composite Superstructure Using a new Assembly Method. Prceedings of the 11th International offshore and Polar Engineering Conference.

26.   Hexel Composites.   Adhgesive Bonding of Honeycomb Structures.   http:// www.heselcomposites.com

27.   E.J. Barbero and L. DeVivo (2001). "A Constitutive Model for Elastic Damage in Fiber- Reinforced PMC Laminae." J. of Damage Mechanics, 10(1) 73–93.

28.   E.J. Barbero and P. Lonetti (2001). "Damage Model for Composites Defined in Terms of Available Data." Mechanics of Composite Materials and Structures, 8(4), 299–315.

29.   D.L. Davidson (1991). "Fracture Characteristics of Al-4% Mg Mechanically Alloyed with SiC Metal. Trans. A. 18A, pp. 2115–2138.

30.   L. Mishnaevsky, M. Dong, S. Honle, and S. Schauder (1999). "Computational Mesomechanics of Particle-Reinforced Composites." Computational Materials Science, v. 16, pp. 133–143.

31.   J. Brockenbrough, W. Hunt, and O. Richmond (1992). "A Reinforced Material Model Using Actual Microstructure Geometry." Scripta Metal. Mater., 27, pp. 385–390.